

**MODIS Algorithm Team (MAT)
Meeting Minutes, 16FEB94**

ATTENDEES:

Abel, Peter
Anuta, Paul
Ardanuy, Phillip
Baden, Joan
Barnes, Bill
Bryant, Tom
Butler, Jim
Che, Nianzeng
Farwell, Lester
Goff, Tom
Goldberg, Larry

Rapporteur

Goodwin, Dave
Guenther, Bruce
Hoyt, Doug
Knight, Edward
Kvaran, Geir
Maxwell, Marvin
McKay, Al
Montgomery, Harry *Chair*
Wolfe, Robert
Ungar, Stephen
Zukowski, Tmitri J.

The next meeting has been scheduled for Wednesday, February 23, 1994, from 9 - 10:30AM, in Building 22, Room G95. Contact Joan Baden for copies of presentations given (286-1378). See attached current scheduled listing of MAT meetings for 1994.

MINUTES

Harry Montgomery reviewed the attached major MAT milestone chart and stated that it will go through updates as the team progresses and issues become more determined and concrete. Tom Bryant gave an update on SBRC Workstation requirements which, at a minimum, we must match to duplicate SBRC's results. Jim Butler gave a talk on Fluorescence, reporting that Labsphere is marketing a new grade of spectralon called "Spacegrade", and JPL and others have already put their orders in. Tim Zukowski presented a brief overview of the ground calibrators and requested more concrete information on the SIS(Spherical Integrating Source). Tom Goff gave a presentation on L-1A product; MCST to SDST deliverables; and SW coding standards.

ACTION ITEMS (ASSIGNED FEB 16, 94) DUE 23FEB94:

| | |
|--------|---|
| 14.MAT | Tom Bryant to prepare a Purchase Request for Henderson's help for Bruce Guenther's signature. |
| 15.MAT | Ken Brown will talk on Crosstalk (20MIN). |
| 16.MAT | Nianzeng Che will talk on SRCA radiometric calibration (20MIN). |
| 17.MAT | Paul Anuta will talk on Solar Diffuser -Part II- (20MIN). |
| 18.MAT | Geir Kavarán will talk on Level 1B Software Prototype Overview meeting after next (30MIN). |

CONCERNS:

- 1.MATC(2/9/94) Phil Ardanuy is concerned that the Antarctic ice cap may disturb the DC restore level on the BB for the visible/near IR bands, due to BB Emissivity being relatively low.
TBA
- 2.MATC(2/9/94) Paul Anuta is concerned that the BRDF of the scan mirror may be a significant modifier of the effective solar diffuser (SD) BRDF.
- 3.MATC(2/16/94) "Space grade" Spectralon may have a strong affinity for hydrocarbons which fluoresce under UV at MODIS wavelengths.
- 4.MATC(2/16/94) MODIS spec does not address polarization in the 2.5 to 5 μm spectral region. We need to make sure SBRC tests fully characterize the polarization response.

MODIS ALGORITHM TEAM MEETING

16 FEBRUARY 1994

- 9:00 MAT SCHEDULE (HARRY MONTGOMERY/ED KNIGHT)
- 9:10 GSFC HW/SW FOR ANALIZING SBRC TEST DATA
(TOM BRYANT)
- 9:20 SOLAR DIFFUSER BRDF STABILITY/FLOUORESCENCE
(JIM BUTLER)
- 9:35 CALIBRATION/GSE SYSTEM (TIM ZUKOWSKI)
- 10:00 1. "L-1A" PRODUCT: THE SDST SCAN CUBE FOR
MODIS,
2. MCST-TO-SDST DELIVERABLES
3. SOFTWARE CODING LANGUAGES AND STANDARDS
(TOM GOFF)
- 10:45 ADJOURN

**OFFICIAL
MODIS ALGORITHM TEAM
(MAT)
SCHEDULED MEETINGS
1994**

| Day | Date | Room | Time |
|-------------|----------------|--------------------|------------------|
| Wed | Feb 2 | BLDG 22/G95 | 9-11AM |
| Wed | Feb 9 | BLDG 22/271 | 9-11AM |
| Wed | Feb 16 | BLDG 22/G95 | 9-11AM |
| Wed* | Feb 23 | BLDG 22/G95 | 9-10:30AM |
| Wed | March 2 | BLDG 22/G95 | 9-11AM |
| Wed* | March 9 | BLDG 16/242 | 9-12PM |
| Wed | March 16 | BLDG 22/G95 | 9-11AM |
| Wed | March 30 | BLDG 22/G95 | 9-11AM |
| Mon | April 4 | BLDG 22/G95 | 9-11AM |
| Mon | April 11 | BLDG 22/G95 | 9-11AM |
| Mon | April 25 | BLDG 22/G95 | 8:30-10AM |
| Mon | May 2 | BLDG 22/G95 | 9-11AM |
| Mon | May 9 | BLDG 22/G95 | 9-11AM |
| Mon | May 16 | BLDG 22/G95 | 9-11AM |
| Mon | May 23 | BLDG 22/G95 | 9-10AM |
| Mon | May 30 | BLDG 22/G95 | 9-11AM |
| Mon | June 6 | BLDG 22/G95 | 9-11AM |
| Mon | June 13 | BLDG 22/G95 | 9-11AM |
| Mon | June 20 | BLDG 22/G95 | 9-11AM |
| Mon | June 27 | BLDG 22/G95 | 9-11AM |
| Wed | July 6 | BLDG 22/G95 | 9-11AM |

*Recently scheduled additions

NOTE: Michael Weinreb/NOAA Calibration Scientist will be the "subject" of the March 9, 1994 MAT meeting from 9-12p.m.

**Behavior of PC HgCdTe
Radiometer Channels**

by I.L. Goldberg

Feb 15, 1994

Behavior Of PC HgCdTe Radiometer Channels

Introduction

The primary intention of this analysis is to explain the non-linear response of photoconductive (PC) HgCdTe detectors as a function of scene radiance when used in instruments similar to meteorological satellite radiometers. The effect of instrument temperature changes on detector responsivity and irradiance from the scene will also be discussed. It is assumed that the detector is viewing earth scenes in the thermal infrared region and that the dynamic radiance range produces only a small amount of non-linear response in the detector output. It is also assumed that the background radiation on the detector is moderate and varies very slowly compared to the changes in signal radiance as the detector scans the scene. These assumptions exclude detector conditions like that of the local oscillator in laser communication instruments where the HgCdTe detector is exposed to very large irradiance levels.

There are two main causes for the non-linear response of PC HgCdTe detectors.

1. Conductivity varies directly with irradiance while the output circuit voltage varies directly with the detector resistivity. The inverse relationship between conductivity and resistivity is a major cause of non-linearity.

2. The photoconductive (PC) lifetime decreases as the irradiance increases (responsivity is directly proportional to PC lifetime).

Both the background and scene irradiance are influenced by the instrument temperature. A change from one instrument temperature to a higher one will increase the background radiant power falling on the detector and thus decrease the HgCdTe responsivity. This will cause a small decrease in the slope of the signal voltage vs. scene radiance calibration curve. The change in detector non-linearity due to this increase in background radiation is very small and is usually not the dominant factor in the observed slope change in the radiometer calibration curve of signal voltage vs scene radiance.

A temperature change in the optical system produces a change in the signal level, i.e. irradiance from the scene. This can cause a greater change in the radiometer output than that from the background radiation change.

- a. In the AVHRR optical system an increase in temperature of 10 K above 283 K causes a decrease in optical transmission τ_{opt} to about $.99 \tau_{opt}$. An increase of 20 K decreases the transmission to about $.97 \tau_{opt}$.

- b. For a constant scene radiance a change in focal length or mirror figure will change the scene irradiance at the detector.

c. Radiometer calibration involves output signal vs scene radiance at various base plate temperatures. A plot of signal output signal vs irradiance at the detector would show much smaller change in the calibration curves at the different temperatures.

Further complications arise when : a) the calibration target is not uniform, accurately temperature monitored, sufficiently black or is large enough to cause temperature gradients in the radiometer; b) the detector temperature control point varies by more than a few tenths of a degree; c) aging causes changes in the optical transmission and detector characteristics. Another problem arises when the amount of background area (solid angle actually) seen by the detector varies with scan mirror position. This will cause a background variation at about the same rate as the scene being scanned. These complications will not be considered in this analysis.

In all that follows it will be assumed that signal voltage increases as irradiance increases.

Definition Of Voltage Responsivity

For simplicity it will be assumed that the irradiance at the detector is monochromatic. The detector responsivity \mathfrak{R} (volts/watt) is defined by

$$\mathfrak{R} = \left| dV_s/dP_s \right|$$

V_s =signal voltage (see Fig. 1)

P_s =signal power incident on detector (W)

| | =absolute value

Applying Ohm's law,

$$\mathfrak{R} = \left| I_B dR/dP_s + R dI_B/dP_s \right| \quad 1$$

I_B =bias current (ampere)

R =detector resistance (ohm)

From Fig. 1 it is evident that

$$I_B = V_B / (R + R_L) \quad 2$$

V_B =bias voltage across detector and load resistor

R_L =load resistor

Therefore,

$$\frac{dI_B}{dP_s} = - \frac{V_B}{(R+R_L)^2} \frac{dR}{dP_s} \quad 3$$

Using this expression the responsivity can be written as

$$\mathfrak{R} = \frac{V_B}{R+R_L} \left(1 - \frac{R}{R+R_L} \right) \left| \frac{dR}{dP_s} \right| \quad 4$$

$$= I_B F_b \left| \frac{dR}{dP_s} \right| \quad 5$$

$$F_b = 1 - R/(R+R_L)$$

Since $R_L \gg R$, $F_b \approx 1$. While F_b is measurably different from 1, its variation with P_s is generally masked by the noise (See Appendix A).

Several of the parameters that responsivity is dependent upon change with irradiance and will be discussed before finding the responsivity variation.

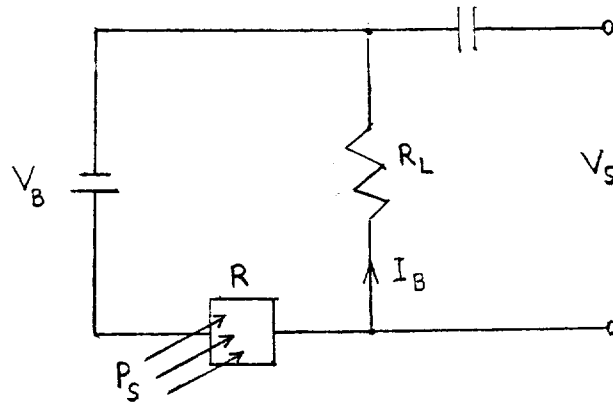


Fig. 1. Simple photoconductor circuit schematic. The signal V_s is taken off the load resistor R_L which is generally much larger than the detector resistance R . As the incident radiant power increases the detector resistance decreases, causing I_B and V_s to increase.

RADIANT SIGNAL LEVEL EFFECTS

Variation Of Resistance With Signal Power

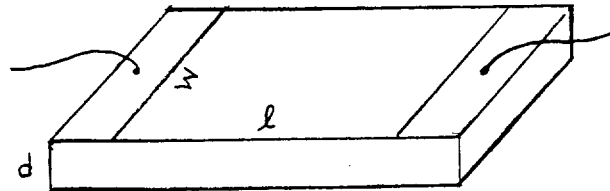


Fig. 2. Detector Geometry

The detector resistance can be expressed by (see Fig. 2)

$$R = \frac{\ell \rho}{wd} = \frac{\ell}{w\sigma d} \quad 6$$

ρ =resistivity (Ohm cm)

σ =conductivity= $1/\rho$

For an n-type PC (usual case for HgCdTe)

$$\sigma = q\mu_e(n_E + n_s) \quad 7$$

q =electron charge= 1.602×10^{-19} coul

μ_e =electron mobility ($\text{cm}^2/\text{V}/\text{sec}$)

n_E =free electron concentration at equilibrium (cm^{-3})

n_s =free electron concentration due to signal (cm^{-3})

While the value of n_E depends on several factors including radiation that comes from the background it is independent of P_s (by definition).

From Eqs. 6 and 7,

$$R = \frac{\ell}{wdq\mu_e(n_E + n_s)} \quad 8$$

The equilibrium resistance R_E is defined as the value of R in the absence of signal irradiance ($n_s=0$).

$$R_E = \frac{\ell}{wdq\mu_e n_E} \quad 9$$

$$\therefore R = R_E / (1 + n_s/n_E) \quad 10$$

$$\frac{dR}{dP_s} = - \frac{R_E}{n_E (1 + n_s/n_E)^2} \frac{dn_s}{dP_s} \quad 11$$

Variation Of n_s With P_s

$$n_s = g_s \tau \quad 12$$

g_s = generation rate of free electron-hole pairs ($\text{cm}^{-3} \text{sec}^{-1}$) due to signal irradiance

τ = photoconductive lifetime (sec)

$$g_s = \frac{\eta Q_s (1 - e^{-\alpha d})}{d} \quad 13$$

η = detector quantum efficiency

Q_s = number of incident signal photons/ cm^2/sec

α = absorption coefficient (cm^{-1})

Except in the neighborhood of and beyond the cut-off wavelength, αd is typically greater than 3 for HgCdTe. Assuming $\alpha d > 3$,

$$g_s \approx \eta Q_s / d \quad 14$$

For monochromatic radiation,

$$Q_s = E_s / (h\nu) = E_s \lambda / (hc) \quad 15$$

E_s = detector signal irradiance (W/cm^2)

h = Planck's constant = 6.626×10^{-34} joule sec

ν = photon frequency (hertz)

λ = photon wavelength (cm)

c = light velocity = 2.998×10^{10} cm/sec

From Eqs. 14 and 15,

$$g_s = \frac{\eta E_s \lambda}{hcd} = \frac{\eta \lambda P_s}{hcw\ell d} \quad 16$$

Using Eq. 12,

$$n_s = \frac{\eta \lambda \tau P_s}{hcw\ell d} \quad 17$$

$$\frac{dn_s}{dP_s} = \frac{\eta \lambda}{hcw\ell d} \left(\tau + P_s \frac{d\tau}{dP_s} \right) \quad 18$$

Variation Of PC Lifetime With Signal Power

Only Auger and radiative lifetimes vary significantly with signal power. The PC lifetime can be expressed in the form

$$1/\tau = 1/\tau_A + 1/\tau_R + 1/\tau_0 \quad 19$$

τ_A =Auger lifetime

τ_R =radiative lifetime

τ_0 =effective lifetime that is insensitive to incident radiation (includes contributions by minority carrier sweepout, surface recombination and Shockley-Read lifetimes)

$$\tau_A = \frac{2n_i^2 \tau_{Ai}}{(n_E + n_s)(n_E + p_E + 2n_s)} \quad 20$$

n_i =intrinsic carrier concentration (cm^{-3})

τ_{Ai} =intrinsic Auger lifetime (sec)

p_E =free hole concentration under equilibrium conditions (cm^{-3})

$$\tau_R = \frac{2n_i \tau_{Ri}}{n_E + p_E + 2n_s} \quad 21$$

τ_{Ri} =intrinsic radiative lifetime (sec)

$$\frac{1}{\tau} = \frac{(n_E + n_s)(n_E + p_E + 2n_s)}{2n_i^2 \tau_{Ai}} + \frac{n_E + p_E + 2n_s}{2n_i \tau_{Ri}} + \frac{1}{\tau_0} \quad 22$$

Differentiating with respect to P_s ,

$$-\frac{1}{\tau^2} \frac{d\tau}{dP_s} = \left(\frac{3n_E + p_E + 4n_s}{2n_i^2 \tau_{Ai}} + \frac{1}{n_i \tau_{Ri}} \right) \frac{dn_s}{dP_s} \quad 23$$

Using Eqs. 20 and 21 and assuming $n_s \ll n_E$

$$-\frac{1}{\tau^2} \frac{d\tau}{dP_s} = \frac{1}{n_E(n_E + p_E)} \left(\frac{3n_E + p_E}{\tau_A} + \frac{2n_E}{\tau_R} \right) \frac{dn_s}{dP_s} \quad 24$$

Let

$$\frac{3}{\tau'} = \frac{1}{n_E + p_E} \left(\frac{3n_E + p_E}{\tau_A} + \frac{2n_E}{\tau_R} \right) \quad 25$$

$$\frac{d\tau}{dP_s} = - \frac{3\tau^2}{n_E \tau'} \frac{dn_s}{dP_s} \quad 26$$

Note that for $n_E \gg p_E$ and $\tau_A \ll \tau_R$ then $\tau' \approx \tau_A$. Also note that $1/\tau' < 1/\tau_A + 1/\tau_R$, so that $\tau' > \tau$.

Using Eqs. 18 and 26,

$$\frac{dn_s}{dP_s} = \frac{\eta\lambda}{hcw\ell d} \left(\tau - \frac{3P_s \tau^2}{n_E \tau'} \frac{dn_s}{dP_s} \right) \quad 27$$

Solving for dn_s/dP_s ,

$$\frac{dn_s}{dP_s} = \frac{y\tau}{1 + 3yP_s \tau^2 / (n_E \tau')} \quad 28$$

where

$$y = \frac{\eta\lambda}{hcw\ell d} \quad 29$$

Using Eq. 28 the lifetime variation can now be written as

$$\frac{d\tau}{\tau} = - \frac{3y\tau^2 dP_s}{n_E \tau' + 3yP_s \tau^2} \quad 30$$

Variation Of Responsivity With Signal Power

Substituting the expression for dn_s/dP_s into Eq. 11 yields

$$\frac{dR}{dP_s} = - \frac{R_E Y \tau}{n_E (1+n_s/n_E)^2 \left[1+3Y P_s \tau^2 / (n_E \tau') \right]} \quad 31$$

Using Eq. 31 the responsivity as given by Eq. 5 becomes,

$$\mathfrak{R} = \frac{F_b I_B R_E Y \tau}{n_E (1+n_s/n_E)^2 \left[1+3Y P_s \tau^2 / (n_E \tau') \right]} \quad 32$$

The equilibrium responsivity \mathfrak{R}_E is defined as the value of \mathfrak{R} as P_s approaches 0, keeping the background radiation constant.

$$\mathfrak{R}_E = F_b I_B R_E Y \tau / n_E \quad 33(a)$$

$$= \frac{\eta \lambda \tau F_b I_B R_E}{hc w \ell n_E d} \quad 33(b)$$

From Eq. 33(a) Y can be expressed as a function of \mathfrak{R}_E .

$$Y = n_E \mathfrak{R}_E / (F_b I_B R_E \tau) \quad 34$$

and the responsivity can be written as

$$\mathfrak{R} = \frac{\mathfrak{R}_E}{(1+n_s/n_E)^2} \left(1 + \frac{3P_s \mathfrak{R}_E \tau}{F_b I_B R_E \tau'} \right)^{-1} \quad 35$$

From Eqs. 17 and 33(b)

$$n_s/n_E = \mathfrak{R}_E P_s / (F_b I_B R_E) \quad 36$$

and \mathfrak{R} can be expressed in the form

$$\mathfrak{R} = \frac{\mathfrak{R}_E}{(1+n_s/n_E)^2} \left(1 + \frac{3n_s \tau}{n_E \tau'} \right)^{-1} \quad 37$$

Since $n_s \ll n_E$ \mathfrak{R} can be approximated as

$$\mathfrak{R} = \frac{\mathfrak{R}_E}{1+2(n_s/n_E)(1+1.5\tau/\tau')} \quad 38$$

Non-Linearity

Since the signal voltage out of the detector is directly proportional to \mathfrak{R} the last term in the denominator of Eq. 38 represents the deviation from linearity. Substituting for n_s/n_E the non-linear term NL becomes

$$NL = 2\mathfrak{R}_E P_s (1 + 1.5\tau/\tau') / (F_b I_B R_E) \quad 39$$

For modest values of P_s the maximum non-linearity (the maximum deviation from a straight line drawn between the origin and the maximum noise-free signal, occurs at $P_M/2$, where P_M is the maximum incident power on the detector in the calibration test (see Fig. 3). This reference non-linearity $(NL)_{ref}$ is

$$(NL)_{ref} = \frac{\mathfrak{R}_E P_M (1 + 1.5\tau/\tau')}{F_b I_B R_E} \quad 40$$

In practice the non-linearity is usually found by comparing the deviations to a least-mean-square (LMS) linear fit of the data. This results in a non-linearity that is approximately half of that given by Eq. 40. For this case the measured value of detector non-linearity $(NL)_D$ is

$$(NL)_D = \frac{\mathfrak{R}_E P_M (1 + 1.5\tau/\tau')}{2F_b I_B R_E} \quad 41$$

The factor $(1 + 1.5\tau/\tau')$ is due to the variation of lifetime with irradiation. The remaining factor is due to the inverse relationship of signal voltage and conductivity change.

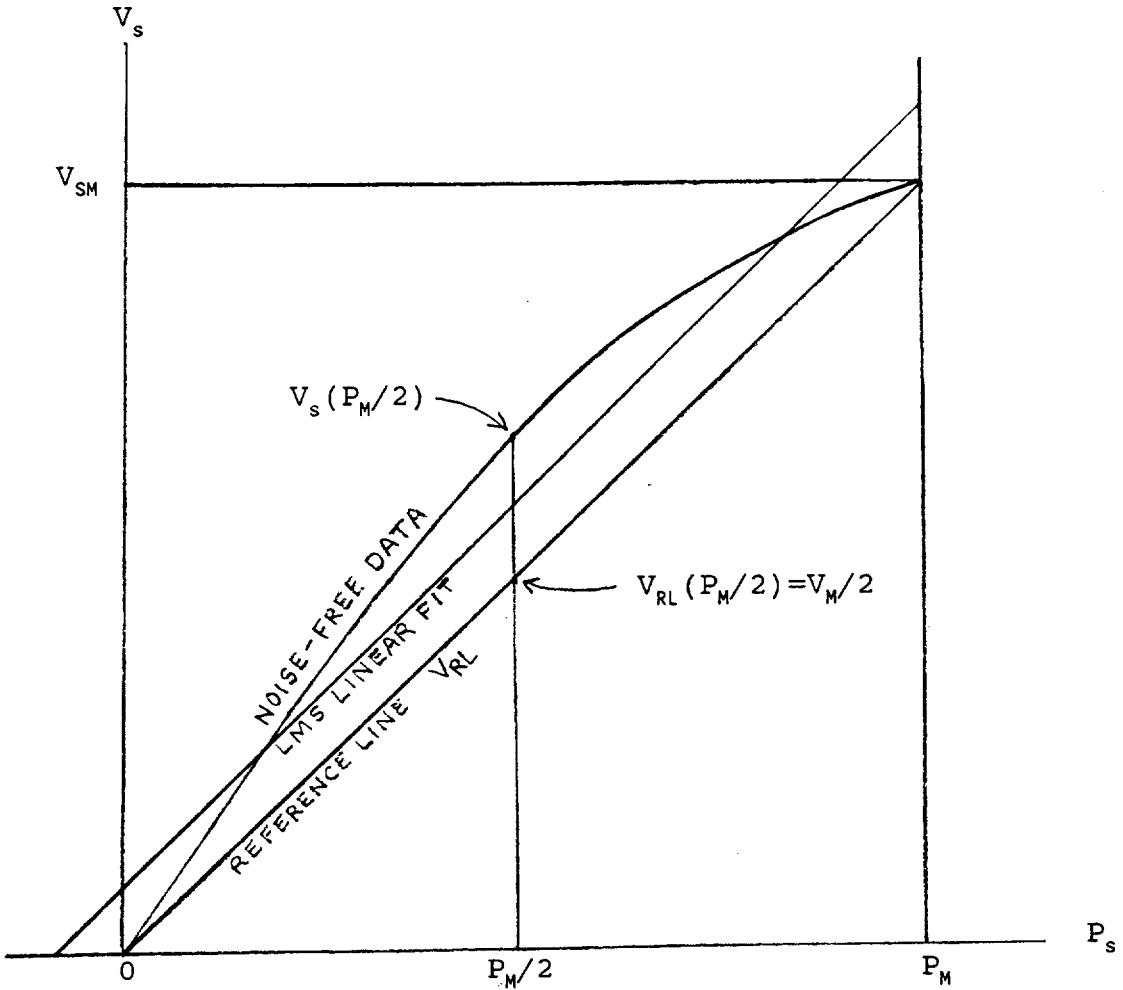
The incident radiant power (P) is related to scene radiance (L in $W/cm^2/sr$) by

$$P = \frac{\pi A_d \tau_{opt} L}{4(f/)^2} \quad 42$$

A_d = detector area or field stop area if employed (cm^2)

τ_{opt} = optical transmission

$f/$ = effective f-number of the spectral channel



V_M = maximum signal voltage
 P_M = maximum incident power
 $(NL)_{ref}$ = reference non-linearity

$$= \frac{V_s(P_M/2) - V_{RL}(P_M/2)}{V_{RL}(P_M/2)}$$

Fig. 3. Detector response curve. V_{RL} is the reference line voltage. For clarity the curvature has been exaggerated. The measured detector non-linearity is with respect to the LMS linear fit and is approximately $.5(NL)_{ref}$. Note that the LMS fit does not pass through the origin.

The variation of incident power with instrument temperature is more involved than indicated by Eq.42. The dependence of transmission on temperature can be estimated from the detailed optical system design (element by element). However the overall effect of a particular temperature change on the detector irradiance (incident radiant power per unit area) is determined empirically (implicitly included in the radiometer calibration at different base plate temperatures) and will vary somewhat from instrument to instrument.

Radiometer calibration normally involves measuring signal output as a function of scene radiance rather than detector signal irradiance. For a fixed scene radiance the detector irradiance will vary with instrument temperature so that the output voltage and non-linearity will change even if the detector responsivity remained constant. Since the changes in the radiometer output voltage due to the changes in the optics and detector are usually in the same direction the slope of the radiometer calibration curve and non-linearity variations with temperature will be greater than that due to the detector alone.

The system non-linearity $(NL)_s$ is measured in a similar manner to that of detector non-linearity, but replacing the V_s vs P_s curve by the radiometer calibration curve of V_s vs L_s . If a LMS quadratic fit to the data is made in the form

$$V = a + bL - cL^2 \quad 43$$

then the non-linearity can be calculated very simply through use of the ratio of the quadratic term divided by the linear term at the maximum radiance value. Call the absolute value of this ratio z . Assuming b and c to be positive,

$$z = cL_M/b \quad 44$$

Then (see appendix B)

$$(NL)_s = \frac{z/4}{1-z} \quad 45$$

As stated in the Introduction the non-linearity is assumed to be small, so z must be significantly less than 1.

INSTRUMENT TEMPERATURE CHANGE EFFECTS

Variation Of Responsivity With Background Radiation

The detector responsivity varies with changing background like that of its variation with signal radiation. However, the temperature changes in a radiometer that are responsible for the background changes can also cause additional variations in the instrument output signal due to the effect that the temperature change has on the optical system. The change in transmission is included in the next section on signal voltage variation with instrument temperature.

From Eqs. 9 and 33(b)

$$\mathfrak{R}_E = \beta \tau / n_E^2 \quad 46$$

$$\beta = \frac{\eta \lambda I_B}{hcw^2 q \mu_e d^2} \quad 47$$

$$\frac{d\mathfrak{R}_E}{dQ_B} = \beta \left(\frac{1}{n_E^2} \frac{d\tau}{dQ_B} - \frac{2\tau}{n_E^3} \frac{dn_E}{dQ_B} \right) \quad 48$$

Q_B = photons/cm²/sec incident on the detector that comes from the background

$$\frac{d\mathfrak{R}_E}{\mathfrak{R}_E} = \frac{d\tau}{\tau} - \frac{2dn_E}{n_E} \quad 49$$

$$n_E = n_0 + \eta Q_B \tau / d \quad 50$$

n_0 = free electron concentration (cm⁻³) with 0 background.

$$\frac{dn_E}{dQ_B} = \frac{\eta}{d} \left(\tau + Q_B \frac{d\tau}{dQ_B} \right) \quad 51$$

$d\tau/dQ_B$ can be found in the same way that was used for finding $d\tau/dP_s$ in Eq. 26.

$$\frac{d\tau}{dQ_B} = - \frac{3\tau^2}{n_E \tau'} \frac{dn_E}{dQ_B} \quad 52$$

Solving for dn_E/dQ_B from Eqs. 51 and 52

$$\frac{dn_E}{dQ_B} = \frac{\eta\tau/d}{1+3\eta Q_B \tau^2 / (n_E \tau' d)} \quad 53$$

Assuming the second term in the denominator to be $\ll 1$,

$$\frac{dn_E}{n_E} = \frac{\eta\tau d Q_B}{n_E d} \quad 54$$

$$\frac{d\tau}{\tau} = - \frac{3\eta\tau^2 d Q_B}{n_E \tau' d} \quad 55$$

Using Eq. 49,

$$\frac{d\mathfrak{R}_E}{\mathfrak{R}_E} = - \frac{2\eta\tau d Q_B}{n_E d} \left(1 + \frac{1.5\tau}{\tau'} \right) \quad 56$$

Signal Voltage Variation With Instrument Temperature

Taking both responsivity and optical transmission into account,

$$d(V_s) = d(\mathfrak{R}_E P_s) = P_s \frac{\partial \mathfrak{R}_E}{\partial Q_B} dQ_B + \mathfrak{R}_E \frac{\partial P_s}{\partial \tau_{opt}} d\tau_{opt} \quad 57$$

The radiant power that reaches the detector that comes from the scene is directly proportional to the optical transmission.

$$\frac{\partial P_s}{\partial \tau_{opt}} = \frac{P_s}{\tau_{opt}}$$

Using Eq. 56,

$$dV_s = - \frac{2\eta\tau \mathfrak{R}_E P_s dQ_B}{\eta_E d} \left(1 + \frac{1.5\tau}{\tau'} \right) + \frac{\mathfrak{R}_E P_s d\tau_{opt}}{\tau_{opt}} \quad 58$$

$$\frac{dV_s}{V_s} = - \frac{2\eta\tau dQ_B}{\eta_E d} \left(1 + \frac{1.5\tau}{\tau'} \right) + \frac{d\tau_{opt}}{\tau_{opt}} \quad 59$$

$$= \frac{d\mathfrak{R}_E}{\mathfrak{R}_E} + \frac{d\tau_{opt}}{\tau_{opt}} \quad 60$$

Note that the second term on the right side of Eq. 60 really represents the optics induced relative change in irradiance when the detector views a constant scene radiance at a different instrument temperature. It is assumed that the electronic amplifiers and processing circuits are unaffected over the temperature range used in the calibration tests.

Variation Of Non-Linearity With Instrument Temperature

The variation of detector non-linearity with background radiation is somewhat smaller than the responsivity variation with background. From Eq 41 it is seen that the non-linearity is proportional to \mathfrak{R}_E/R_E so that $(NL)_D$ is proportional to τ/n_E whereas \mathfrak{R}_E is proportional to τ/n_E^2 . This leads to

$$\frac{d(NL)_D}{(NL)_D} = \frac{d\tau}{\tau} - \frac{dn_E}{n_E} \quad 61$$

When the temperature effect on the optical system is included then the term $d\tau_{opt}/\tau_{opt}$ must be added to Eq. 61.

Using Eqs. 53 and 54

$$\frac{d(NL)_D}{(NL)_D} = - \frac{\eta\tau dQ_B}{n_E d} \left(1 + \frac{3\tau}{\tau'} \right) + \frac{d\tau_{opt}}{\tau_{opt}} \quad 62$$

Because the non-linearity is normally very small and also because of the uncertainty of the numerical value of the last term in the above equation it is difficult to predict with any accuracy the value of the change in non-linearity as a function of instrument temperature in advance of experimental results on the behavior of the optical system.

Variation Of Resistance With Background

Changes in the background radiation affect the resistance of the detector by changing its equilibrium free electron concentration.

$$R_E = \gamma/n_E \quad 63$$

where $\gamma = \ell/(wq\mu_e d)$

$$\frac{dR_E}{dQ_B} = - \frac{\gamma}{n_E^2} \frac{dn_E}{dQ_B} = - \frac{R_E}{n_E} \frac{dn_E}{dQ_B} \quad 64$$

Using Eq. 54,

$$\frac{dR_E}{dQ_B} = - \frac{\eta \tau R_E}{n_E d} \quad 65(a)$$

or

$$\frac{dR_E}{R_E} = - \frac{\eta \tau d Q_B}{n_E d} \quad 65(b)$$

To illustrate the order of magnitude of this change, data from AVHRR FM 101 will be used.

$$R_E = 73.3 \text{ ohms @ } T_{\text{bkg}} = 283 \text{ K}$$

$$\eta = .82$$

$$\tau = 4.6 \times 10^{-7} \text{ s}$$

$$dQ_B = 4.5 \times 10^{15} \text{ phot/cm}^2/\text{s} \text{ (283 K to 293 K)}$$

$$n_E = 1 \times 10^{15} \text{ cm}^{-3}$$

$$d = .001 \text{ cm}$$

$$dR_E = - .124 \text{ ohm} \quad (283 \text{ K to } 293 \text{ K})$$

Appendix A

Variation of F_b with P_s

$$F_b = 1 - R_L/(R+R_L) = R_L/(R+R_L) \quad A1$$

$$\frac{dF_b}{dP_s} = - \frac{R_L}{(R+R_L)^2} \frac{dR}{dP_s}$$

$$= - \frac{F_b}{R+R_L} \frac{dR}{dP_s} \quad A2$$

From Eq.30, Assuming n_s/n_E and $3\gamma P_s \tau^2 / (n_E \tau')$ are small,

$$\frac{dR}{dP_s} = - \frac{R_E \gamma \tau}{n_E} \quad A3$$

Using Eq.33,

$$dR/dP_s = \mathfrak{R}_E / (F_b I_B) \quad A4$$

$$\therefore \frac{dF_b}{dP_s} = \frac{\mathfrak{R}_E}{I_B (R+R_L)} \quad A5$$

Using Eq.A1,

$$\frac{dF_b}{F_b} = \frac{\mathfrak{R}_E dP_s}{R_L I_B} \quad A6$$

From AVHRR FM 101 data: $\mathfrak{R}_E=14,300$ V/W, $I_B=.003$ A,

$R=73.3$ ohms, $R_L=4930$ ohms, $dP_s=2.28 \times 10^{-7}$ W.

$$F_b = .9853$$

$$dF_b/F_b = 2.2 \times 10^{-4}$$

$$dF_b = 2.17 \times 10^{-4}$$

Appendix B

System non-linearity

Assume the LMS quadratic fit to the calibration data to be

$$V_Q = a + bL - cL^2 \quad B1$$

At the maximum scene radiance L_M ,

$$V_M = a + bL_M - cL_M^2 \quad B2$$

The equation of the straight line V_L joining the end points is (see Fig. 4)

$$\begin{aligned} V_L &= a + L(V_M - a)/L_M \\ &= a + (b - cL_M)L \end{aligned} \quad B3$$

When $L = L_M/2$ the values of V on the parabola and straight line are

$$V_Q(L_M/2) = a + (b - cL_M/2)L_M/2 \quad B4$$

$$V_L(L_M/2) = a + (b - cL_M)L_M/2 \quad B5$$

The reference non-linearity is defined by

$$(NL)_{ref} = \frac{V_Q(L_M/2) - V_L(L_M/2)}{V_L(L_M/2) - a} \quad B6$$

Using the expressions in Eqs. B4 and B5

$$(NL)_{ref} = \frac{cL_M/2}{b - cL_M} \quad B7$$

Letting $z = cL_M/b$ B8

$$(NL)_{ref} = \frac{z/2}{1 - z} \quad B9$$

Remembering that the non-linearity with respect to a LMS linear fit is half of $(NL)_{ref}$,

$$(NL)_s = \frac{z/4}{1 - z} \quad B10$$

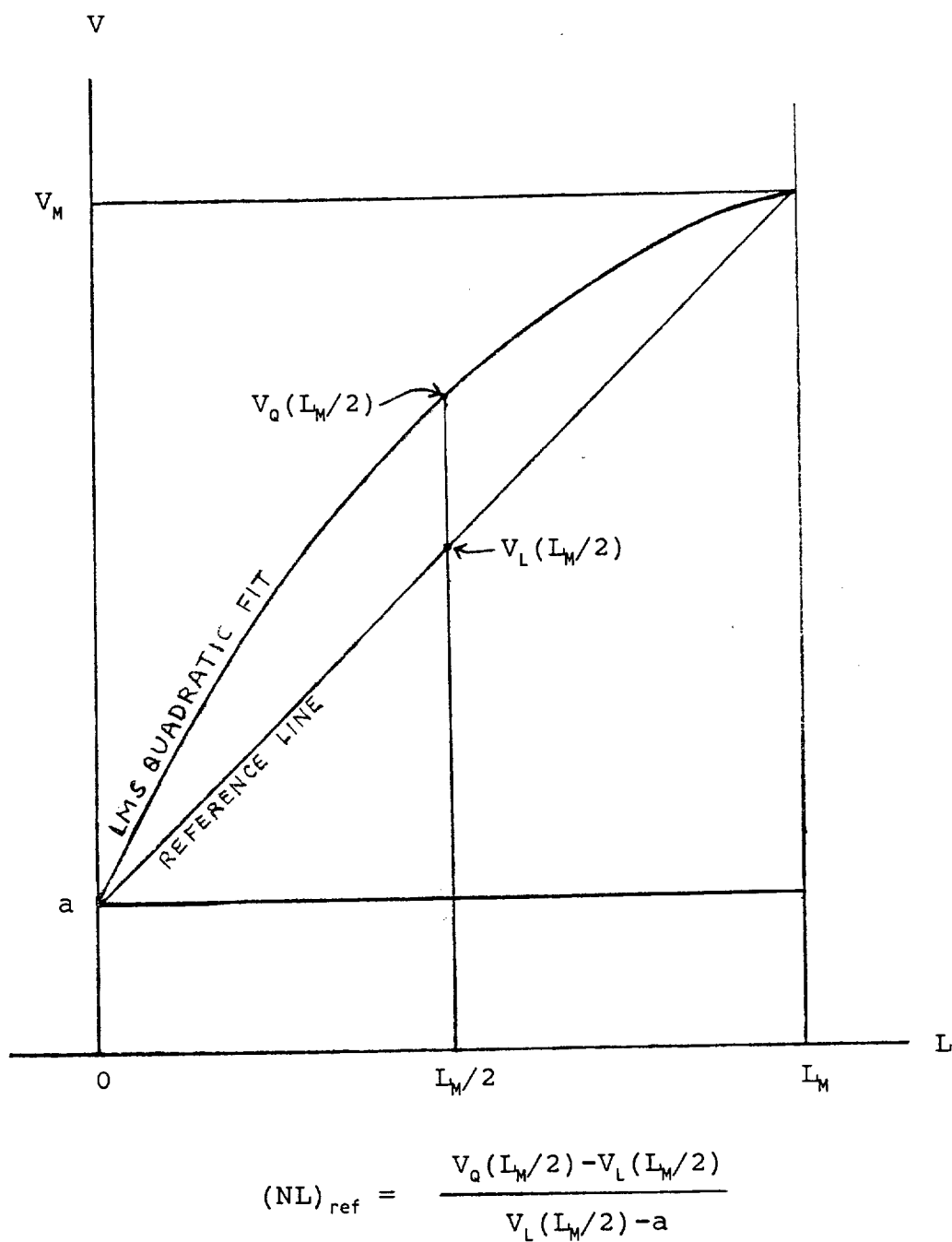


Fig. 4. System response curve. $(NL)_S = .5(NL)_{\text{ref}}$.

Summary

1. Variation of detector responsivity \mathfrak{R} with incident signal power P_s

$$\mathfrak{R} = \frac{\mathfrak{R}_E}{1 + 2(n_s/n_E)(1 + 1.5\tau/\tau')}$$

$$n_s/n_E = \frac{\mathfrak{R}_E P_s}{F_b I_B R_E}$$

\mathfrak{R}_E =equilibrium responsivity (V/W)

I_B =bias current (A)

R_E =equilibrium detector resistance (ohms)

τ =photoconductive lifetime (sec)

τ' =effective irradiance sensitive lifetime (sec) = Auger lifetime

n_s =free electron concentration (cm^{-3}) due to signal

n_E =free electron concentration (cm^{-3}) at equilibrium

R_L =load resistance (ohms)

F_b = bridge factor = $R_L / (R_E + R_L)$

2. Variation of responsivity with background

$$\frac{d\mathfrak{R}_E}{\mathfrak{R}_E} = - \frac{2\eta\tau dQ_B}{n_E d} \left(1 + \frac{1.5\tau}{\tau'} \right)$$

η =detector quantum efficiency

dQ_B =change in incident photon flux density due to background change ($\text{phot}/\text{cm}^2/\text{sec}$)

d =detector thickness (cm)

3. Variation of detector resistance with background

$$\frac{dR_E}{R_E} = - \frac{\eta\tau dQ_B}{n_E d}$$

4. Signal (V_s) variation with instrument temperature

$$\frac{dV_s}{V_s} = \frac{d\mathfrak{R}_E}{\mathfrak{R}_E} + \frac{d\tau_{opt}}{\tau_{opt}}$$

τ_{opt} =optical transmission

5. Detector non-linearity

$$(NL)_D = \frac{\mathfrak{R}_E P_M (1 + 1.5\tau/\tau')}{F_b I_B R_E}$$

P_M =maximum incident radiant power (W)

$(NL)_D$ is the maximum non-linearity from a LMS linear fit of the data.

6. System non-linearity

Assume the LMS quadratic fit to be

$$V_q = a + bL - cL^2$$

$$(NL)_S = \frac{z/4}{1-z}$$

where,

$$z = cL_M/b$$

L_M =maximum scene radiance (W/cm²/sr)

Latest Developments On the Problem of Spectralon Fluorescence

J.J. Butler
February 16, 1994

Latest Developments On the Problem of Spectralon Fluorescence

-A concern has been voiced by several members of the MAT concerning the undesirable property of Spectralon fluorescing in blue wavelengths under ultraviolet illumination.

Latest Developments On the Problem of Spectralon Fluorescence (con't.)

-A conversation on February 14 with Art Springsteen of Labsphere (a.k.a. the Guru of Spectralon) revealed the following information concerning steps Labsphere is taking to attack the problem of Spectralon fluorescence:

1. Labsphere is preparing to market a new "grade" of Spectralon termed "Space Grade" which reportedly does not fluoresce under uv light. They are currently taking advance orders for this grade. MISR/JPL and MERIS have already expressed their desire for this grade of Spectralon. It is more costly than the optical grade Spectralon due to the painstaking processes needed to prepare it.

2. The new process for preparing "Space Grade" Spectralon includes:

- vacuum baking the PTFE resin,**
- molding/pressing/scinterring/machining the solid Spectralon,**
- ultrasonically cleaning the Spectralon in ultrapure ethanol,**
- vacuum baking the Spectralon again,**
- packaging the Spectralon in special, non-contaminating containers.**

Latest Developments On the Problem of Spectralon Fluorescence (con't.)

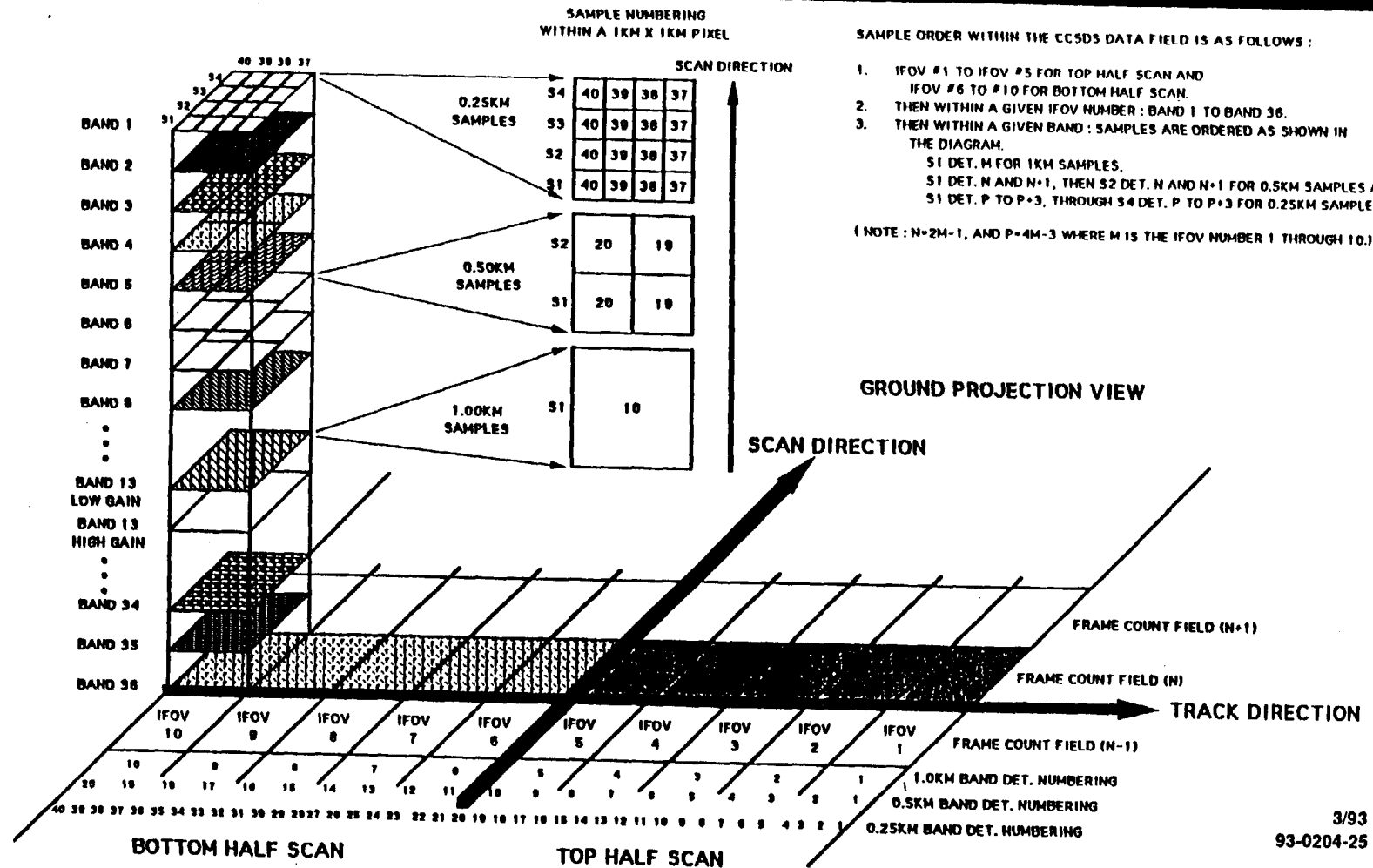
- 3. The fluorescing molecule according to Springsteen and Al Steigman of JPL is probably a saturated, straight-chain C_{14} to C_{16} hydrocarbon very similar to lubricating oil.**
- 4. You may ask, "Well, where does this hydrocarbon come from?" According to Springsteen, the resin is manufactured by Dupont/ICI Americas in a reaction vessel the size of a football field and approximately three feet deep. They fill the vessel with water and add sodium peroxydisulfate. They then bubble tetrafluoroethylene through this solution and out precipitates the PTFE. The water is sucked out of the vessel and the PTFE is dried. It is then chopped up and marketed as the resin. At some point in this manufacturing process, the hydrocarbon is being introduced.**
- 5. Art Springsteen is sending me more detailed information on "Space Grade" Spectralon and how it is prepared.**



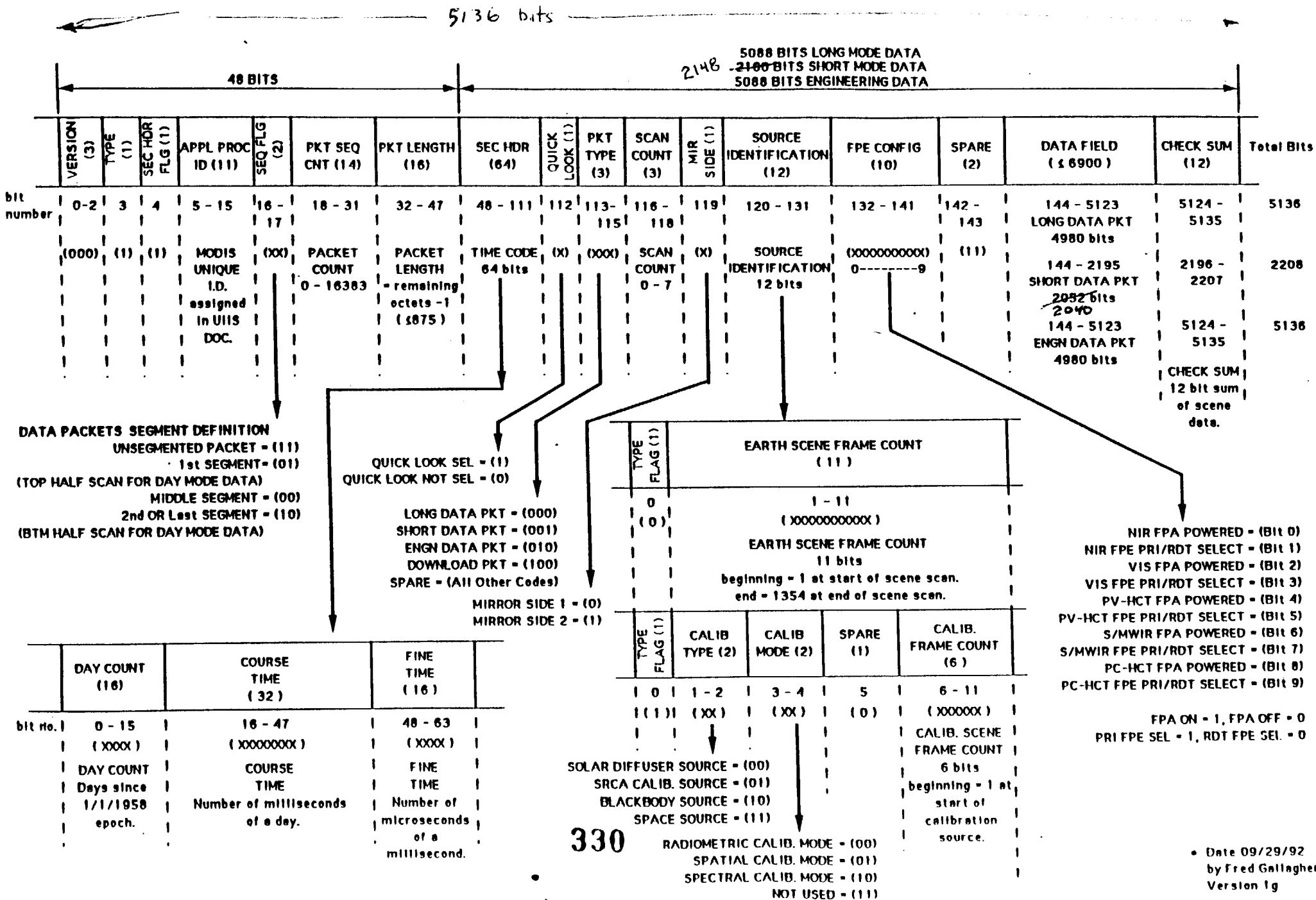
MODIS SCIENCE DATA SWATH AND SAMPLE NUMBERING DEFINITION



SANTA BARBARA RESEARCH CENTER
a subsidiary



Detailed CCSDS Science Data Format.

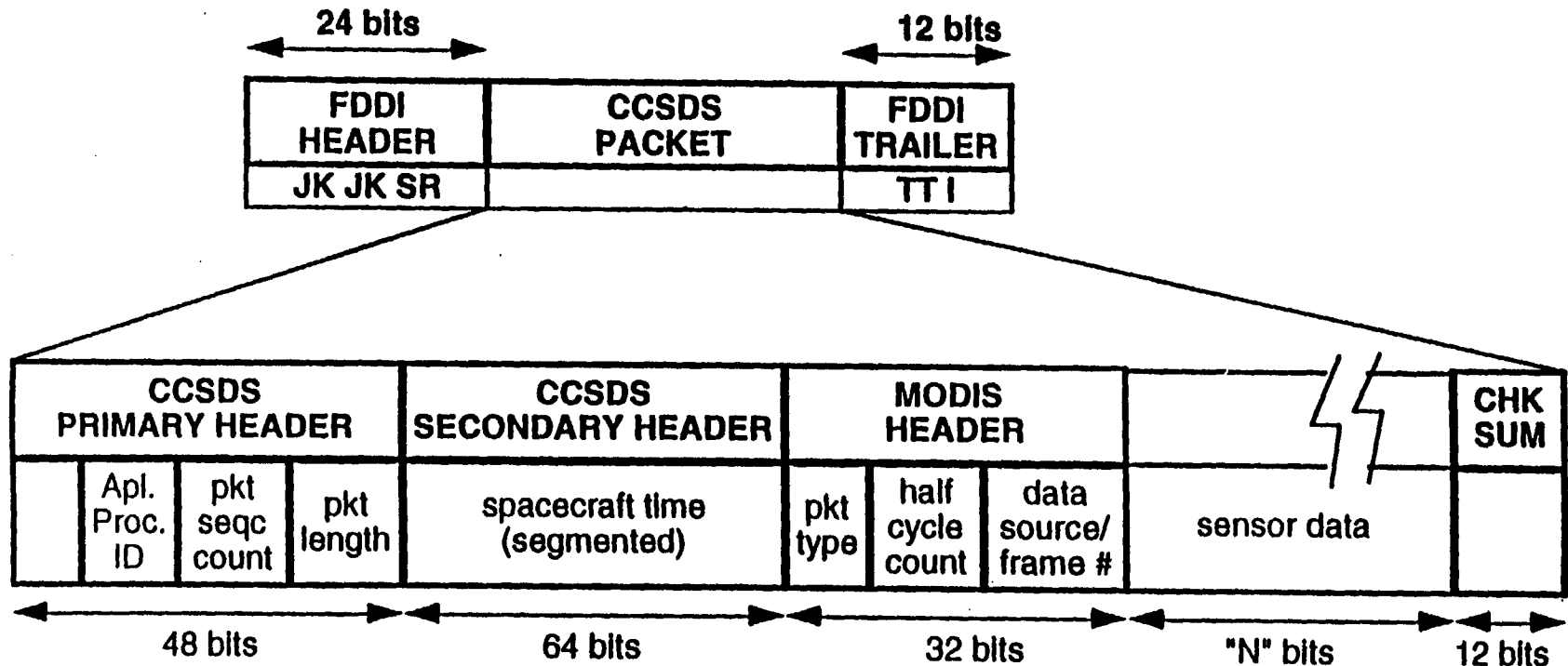




SCIENCE DATA PACKETS



SANTA BARBARA RESEARCH CENTER
a subsidiary



- **LONG PACKETS (All bands):** $N = 5 \text{ IFOVs} \times 83 \text{ samples} \times 12 \text{ bits} = 4980$
- **SHORT PACKETS (Bands 20 through 36):** $N = 10 \text{ IFOVs} \times 17 \text{ samples} \times 12 \text{ bits} = 2040$

Mission Statement

Given: PRELAUNCH TESTING, and DATA SYSTEMS (FORMAT/TIMING)

Interpretation to Date:

Review calibration plans, procedures, and hardware documentation.

Verify system level adequacy for MODIS calibration goals.

Identify potential problems for in-flight calibration resulting from ground procedures.

Identify gaps in ground calibration plans.

Learn whatever is necessary to support the implementation of data analysis by MAT in support of in-flight calibration algorithm development/validation.

Become familiar with hardware, software, and test procedures (S/W level) from users' point of view.

Review algorithm development from implementation point of view.

Establish the means of retrieving SBRC generated test data.

HUGHES

SANTA BARBARA RESEARCH CENTER
a subsidiary

SYSTEM PERFORMANCE TEST MATRIX



| TEST PARAMETER | SPEC PARA | TEST ENVIRONMENT | Scan mirror status | GSE optical slits |
|-------------------------|-----------|------------------|--------------------|----------------------|
| Spatial - IFOV | 3.3.1 | Amb lab | non-scanning | IAC with slits |
| Response uniformity | 3.4.5.4 | | | |
| Spectral | 3.3.3 | Amb lab & T/V | non-scanning | MGBC+monochromator |
| wavelength tolerance | 3.3.3.2 | Amb lab & T/V | | |
| out of band ripple | 3.3.3.3 | Amb lab | | |
| wavelength stability | 3.3.3.4 | Amb lab & T/V | | |
| wavelength accuracy | 3.4.7.4 | Amb lab & T/V | | |
| | 3.4.7.5 | Amb lab & T/V | | |
| Polarization | 3.3.5 | Amb lab | non-scanning | MGBC+polarizer prism |
| MTF | 3.4.2 | Amb lab & T/V | scanning | MGBC+slits |
| Transient response | 3.4.4 | Amb lab | scanning | MGBC+reticles |
| Radiometric performance | 3.4.5 | Amb lab & T/V | scanning | SIS (100) & BCS |
| Dynamic range | 3.4.1 | | | |
| SNR | 3.4.1 | | | |
| System noise meas | 3.4.5.5 | | | |
| Ch to ch uniformity | 3.4.5.3.2 | | | |
| System noise | 3.4.5.5 | | | |
| System crosstalk | 3.4.5.3.3 | Amb lab | scanning | MGBC+wide slits |
| Ghosting | | Amb lab | scanning | MGBC+full aperture |
| Geometric performance | 3.4.6 | | | |
| Pointing knowledge | 3.4.6.1 | Amb lab | non-scanning | MGBC+plg assy |
| Alignment change | 3.4.6.2 | Amb lab | non-scanning | MGBC+plg assy |
| Spectral Band Req. | 3.4.6.3 | Amb lab & T/V | scanning | MGBC+SBR reticles |
| Radiometric stability | 3.4.7 | | scanning | |
| short term | 3.4.7.1 | Amb lab | | SIS(100) & BCS |
| long term | 3.4.7.2 | analysis | | NA |
| spectral band to band | 3.4.7.3 | Amb lab & T/V | | SIS(100) & BCS |
| Sray light | 3.4.8 | Amb lab | scanning | |
| Direct sunlight | 3.4.8.1 | Amb lab | | Solar Test Source |
| Bright target | 3.4.8.2 | Amb lab | | SIS(100) |
| Dark target | 3.4.8.3 | Amb lab | | SIS(100) |
| Warm target | 3.4.8.4 | Amb lab | | MGBC-target reticle |

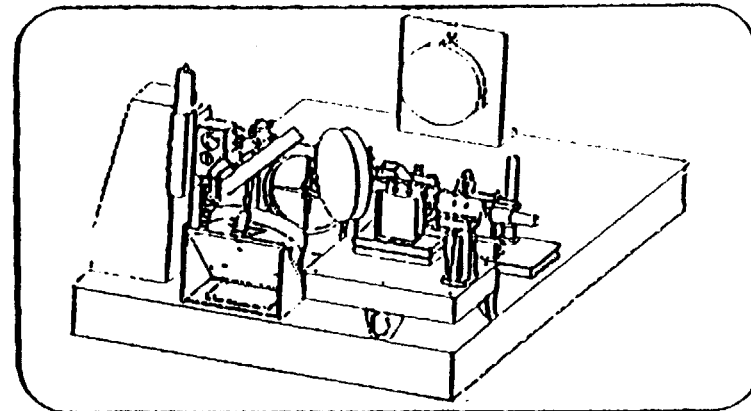
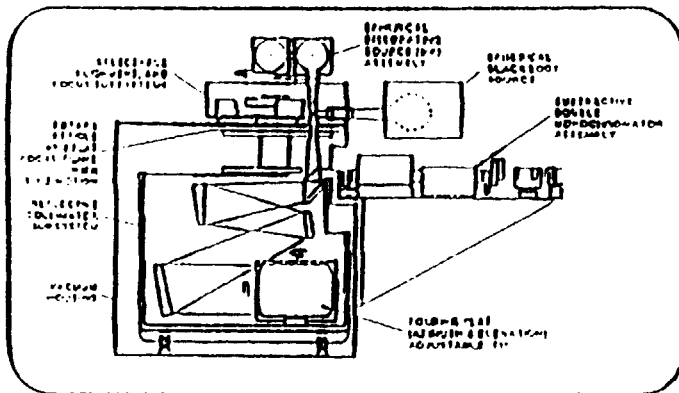


THERE ARE FOUR GSE OPTICAL STIMULUS ASSEMBLIES

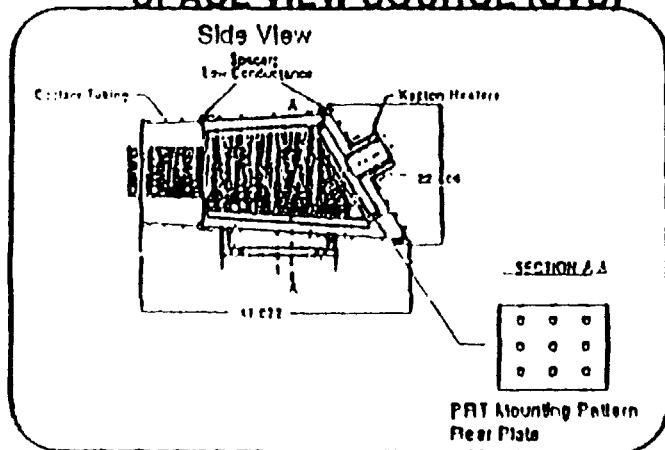


SANTA BARBARA RESEARCH CENTER
A Subsidiary

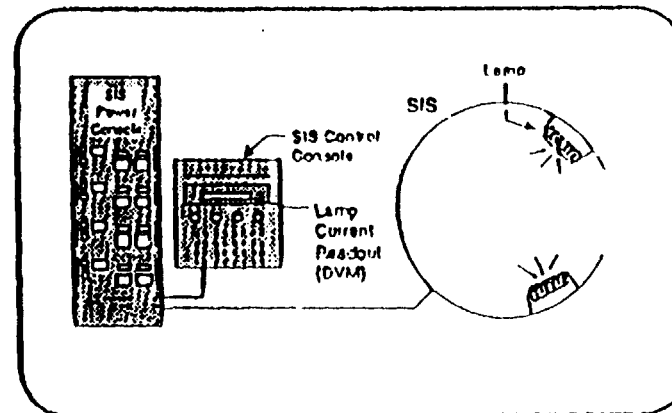
MODIS GROUND BASED CALIBRATOR (MGBC) INTEGRATION & ALIGNMENT COLLIMATOR (IAC)



BLACKBODY CALIBRATION SOURCE (BCS) SPACE VIEW SOURCE (SVS)



SPHERICAL INTEGRATING SOURCE (SIS 100)

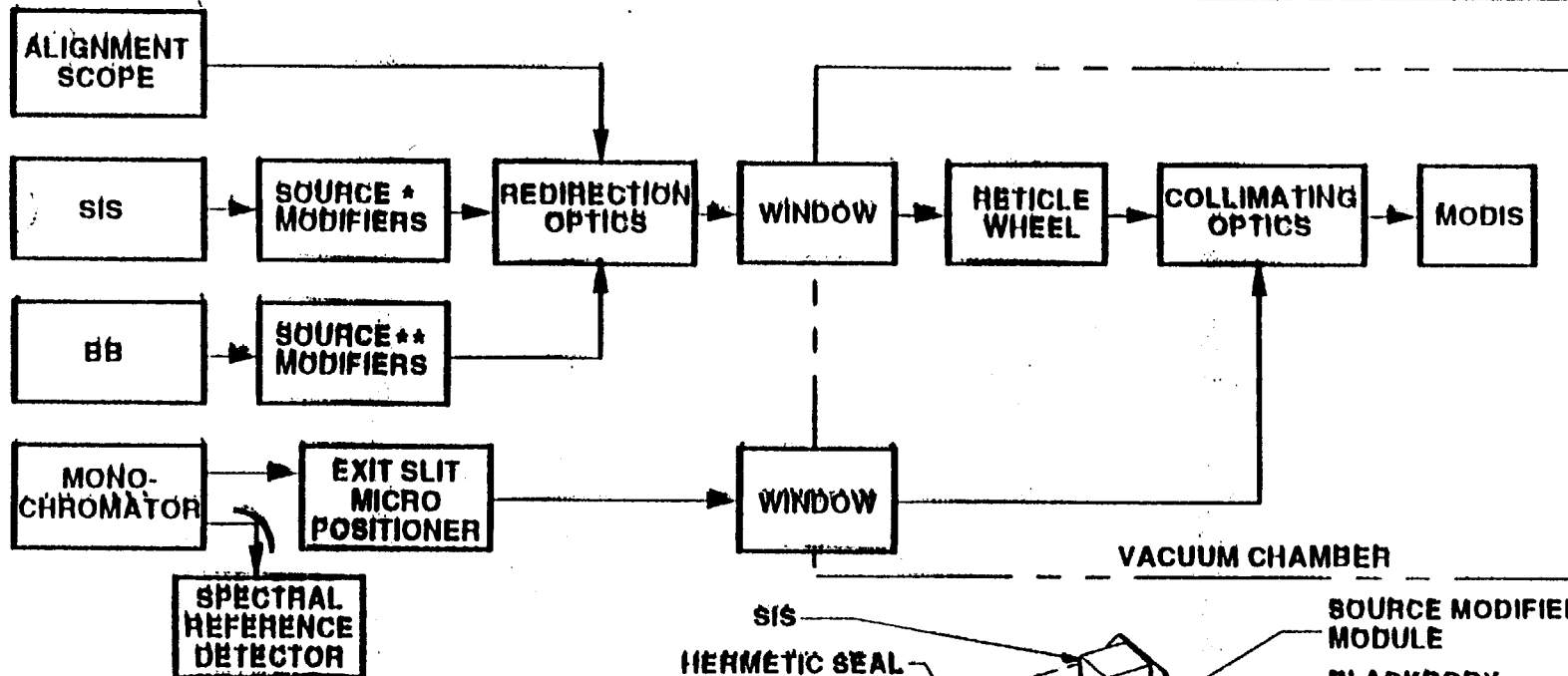




MGBC FUNCTIONAL FLOW DIAGRAM

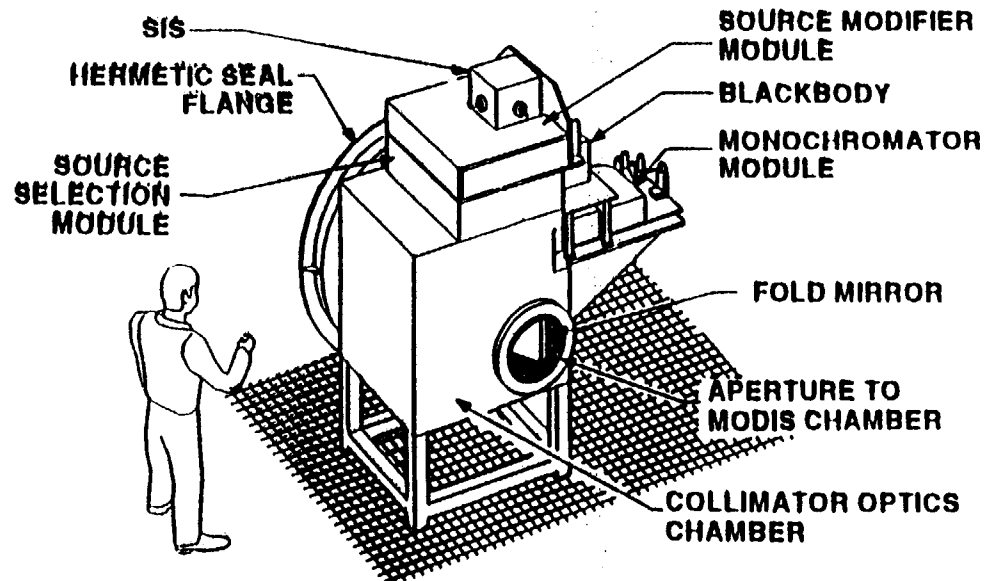


SANTA BARBARA RESEARCH CENTER
a subsidiary



* POLARIZER
NEUTRAL DENSITY FILTERS
SPECTRAL SHAPING FILTERS

** SPECTRAL SHAPING FILTERS



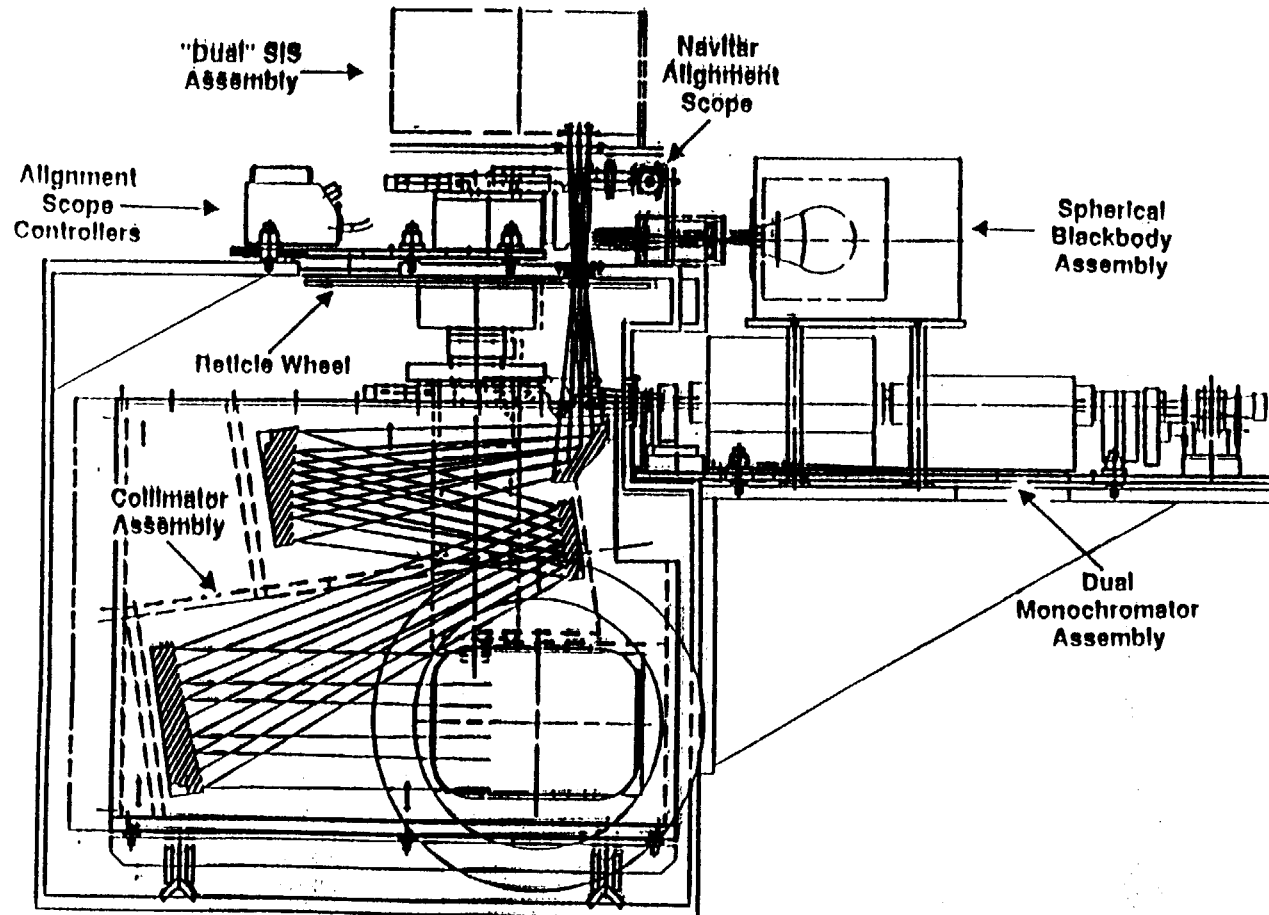
COMPLETE PERSPECTIVE OF CALIBRATOR



MGBC OPTICAL SCHEMATIC DRAWING



SANTA BARBARA RESEARCH CENTER
a subsidiary





SPECTRAL MEASUREMENTS SYSTEM ASSEMBLY LAYOUT



SANTA BARBARA RESEARCH CENTER
SANTA BARBARA RESEARCH CENTER
a subsidiary

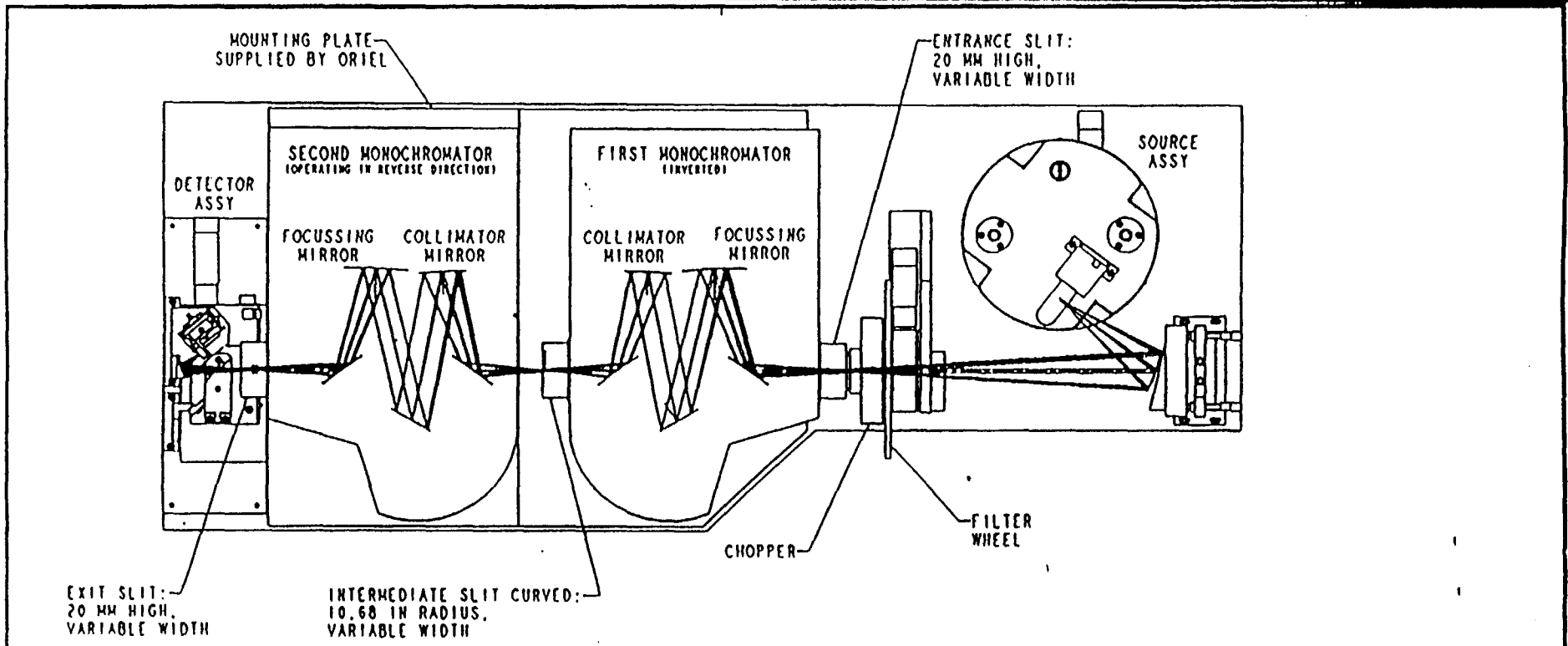


TABLE I

| | SPECTRAL DIMENSIONS HEIGHT (mm) | SPECTRAL DIMENSIONS WIDTH (mm) | SHAPE | MATERIAL |
|---------------------|---------------------------------|--------------------------------|---------|-----------------------|
| GRATINGS | 52 | 57 | | |
| COLLIMATING MIRRORS | 68 | 58 | TOROIDS | ALUM/MgF ₂ |
| FOCUSING MIRROR | 55 | 80 | TOROIDS | ALUM/MgF ₂ |

TABLE II, GRATINGS

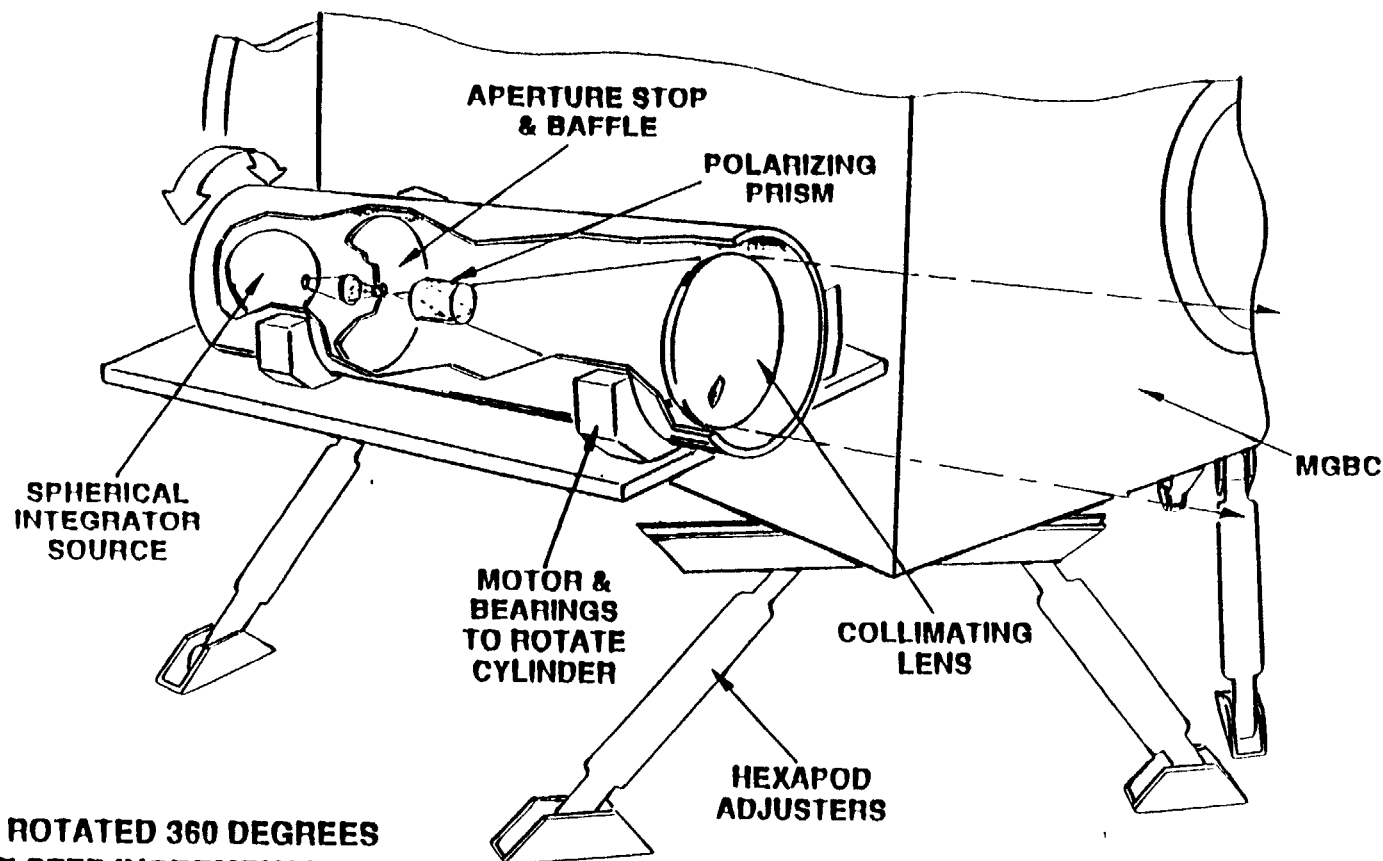
| g/mm | nm | MANUFACTURER | λ |
|------|--------|--------------|----------------|
| 1200 | 400 | ORIEL | 400nm - 15.5um |
| 600 | 1500 | ISA | 400nm - 15.5um |
| 150 | 4000 | ORIEL | 400nm - 15.5um |
| 75 | 12,000 | ISA | 400nm - 15.5um |



MODIS POLARIZANCE IS CHARACTERIZED WITH A STAND-ALONE POLARIZER SUBSYSTEM



SANTA BARBARA RESEARCH CENTER
a subsidiary



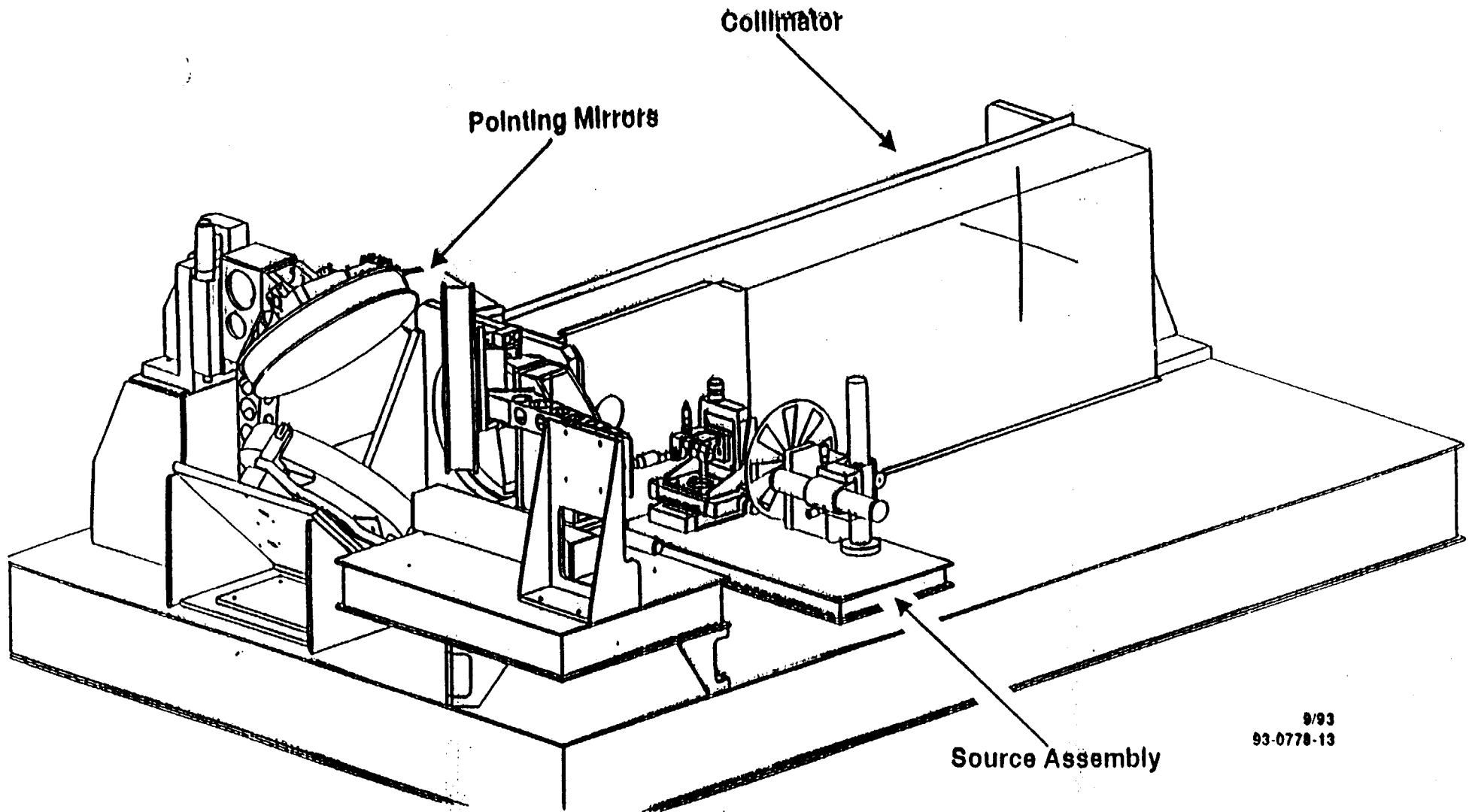
- CYLINDER IS ROTATED 360 DEGREES IN 15 DEGREE STEP INCREMENTS



INTEGRATION AND ALIGNMENT COLLIMATOR DESIGNS NEARLY COMPLETE

HUGHES

SANTA BARBARA RESEARCH CENTER
a subsidiary



9/93
93-0778-13

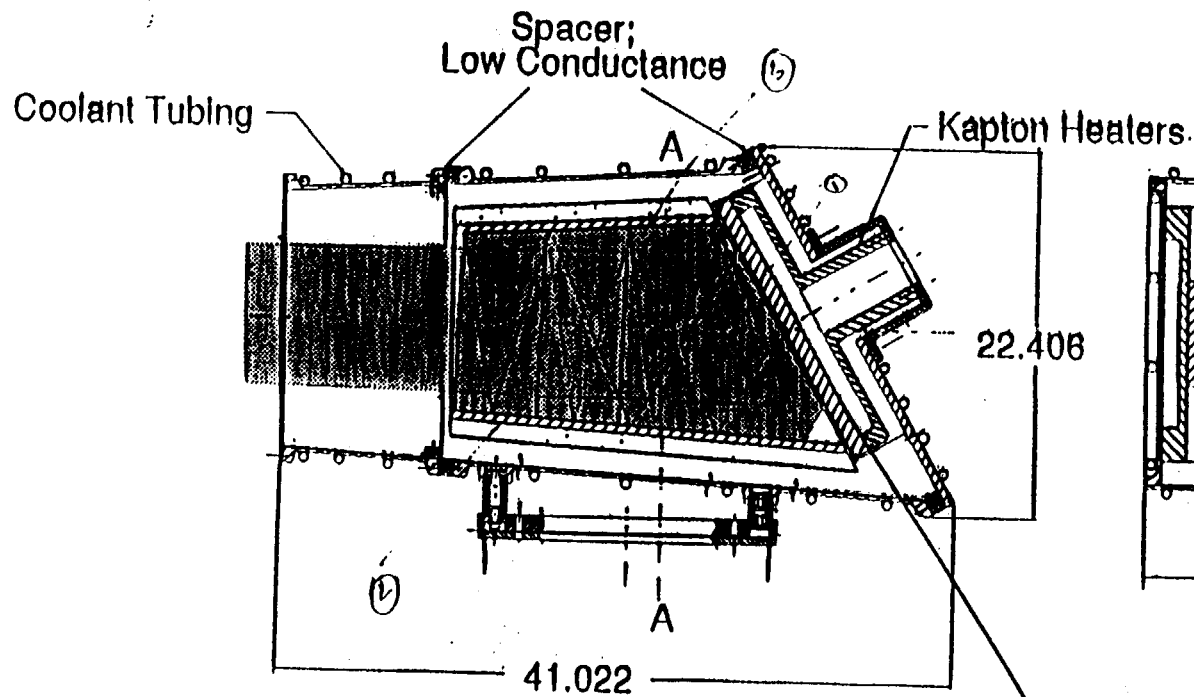


BCS/SVS MECHANICAL DESIGN

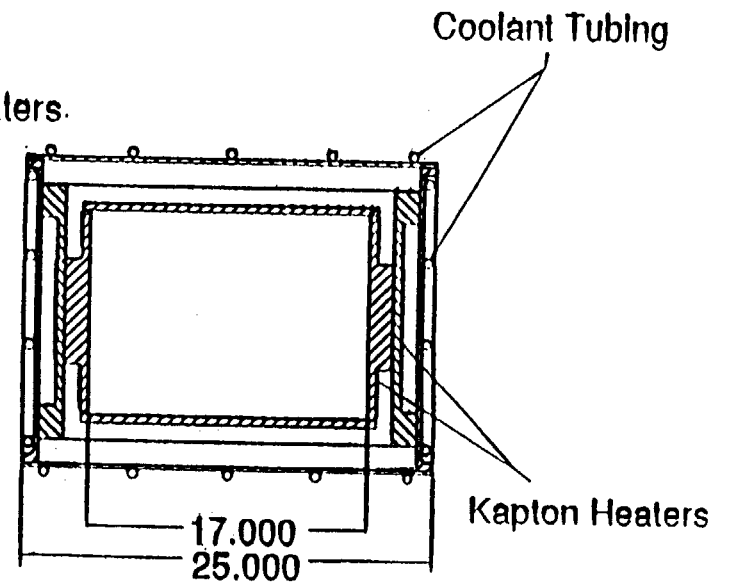


SANTA BARBARA RESEARCH CENTER
a subsidiary

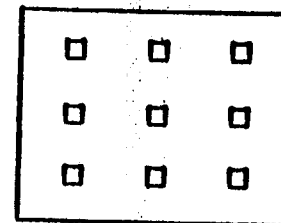
Side View



Front View



SECTION A-A



PRT Mounting Pattern Rear Plate



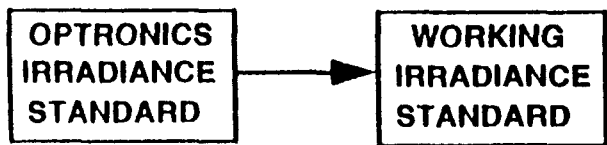
SIS(100) CALIBRATION PLAN



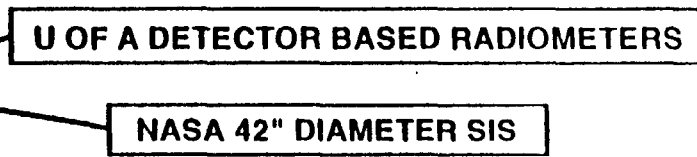
SANTA BARBARA RESEARCH CENTER
a subsidiary

CALIBRATION PATH

SBRC NIST TRACEABLE CALIBRATION



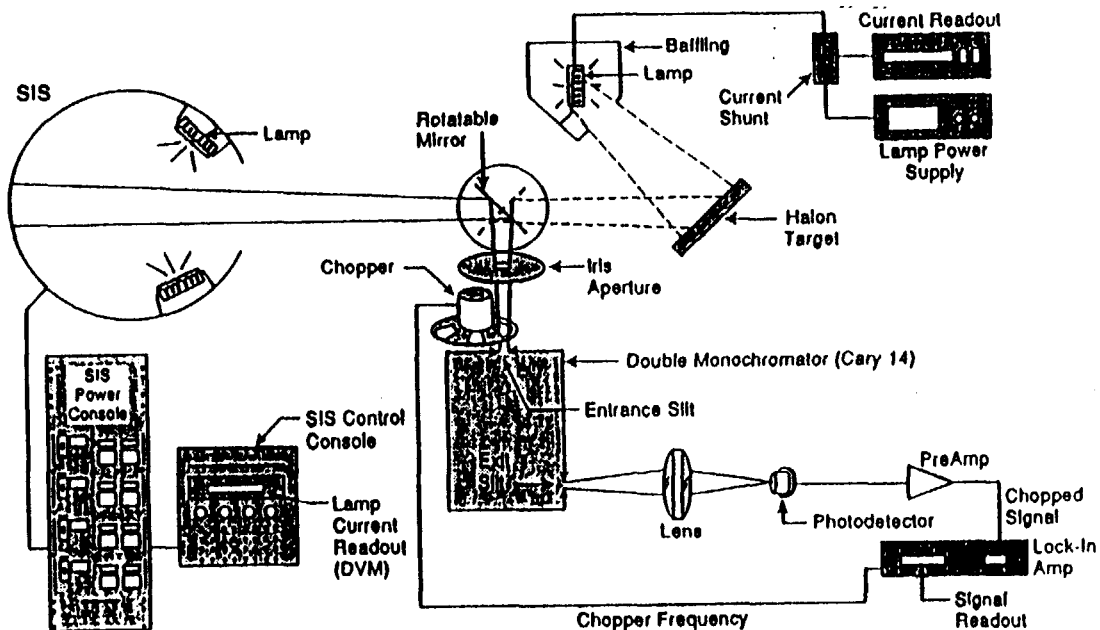
CROSS CALIBRATION



CALIBRATION PLAN

- CROSS-CALIBRATION WITH NASA SIS NOV'92
- SEAWIFS CALIBRATION 0.4 TO 0.9 μm MAR'93
- CROSS-CALIBRATION WITH U OF A DETECTOR JUN'93
- FIRST CALIBRATION FULL RANGE 0.4 TO 2.2 μm JAN'94
- SECOND CALIBRATION FULL RANGE 0.4 TO 2.2 μm SEP'94

SIS(100) CALIBRATION SCHEMATIC

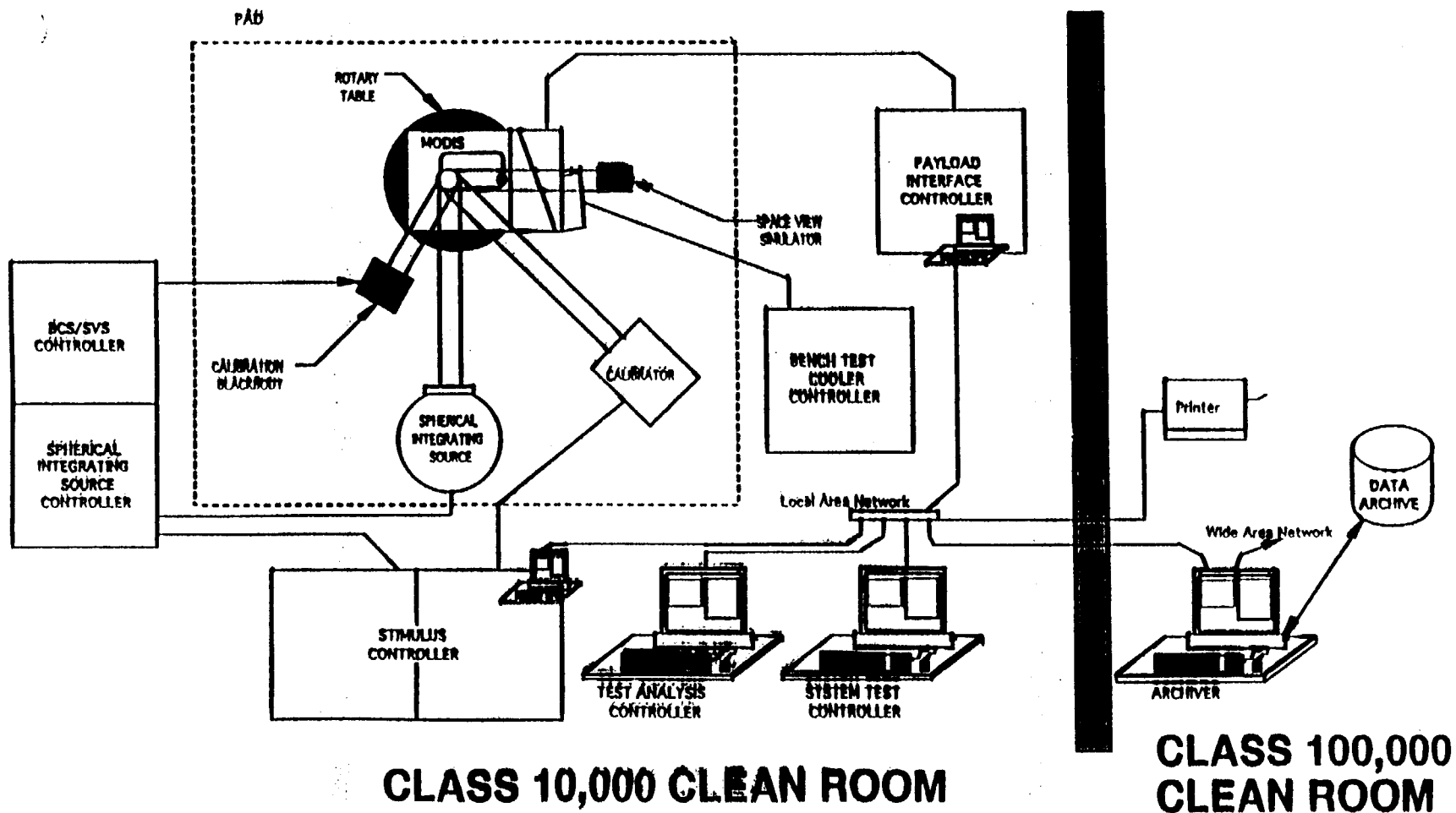




PROPOSED GSE AMBIENT TEST TOPOLOGY

HUGHES

SANTA BARBARA RESEARCH CENTER
a subsidiary

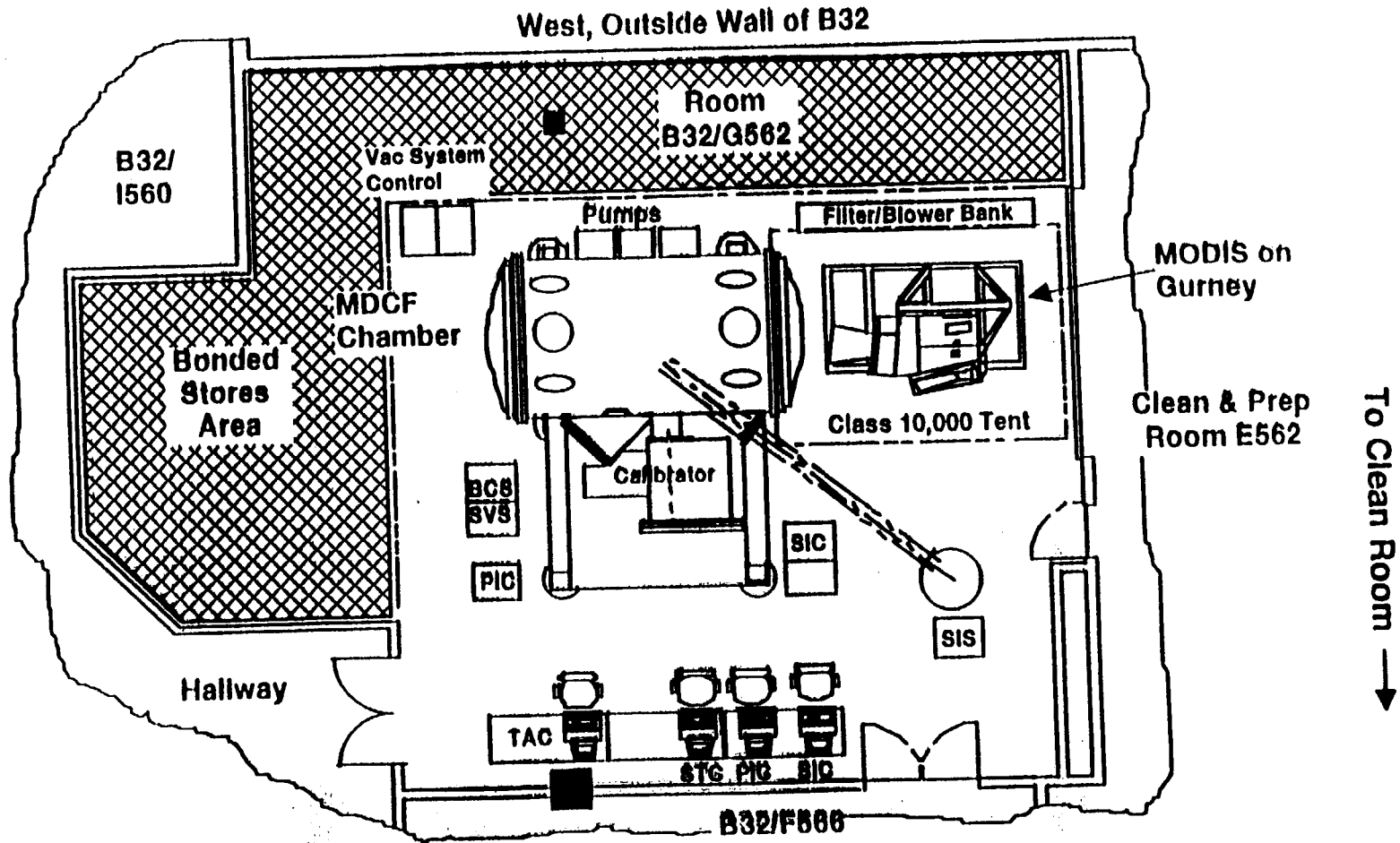




MODIS DEDICATED CALIBRATION FACILITY PROPOSED LAYOUT



SANTA BARBARA RESEARCH CENTER
a subsidiary

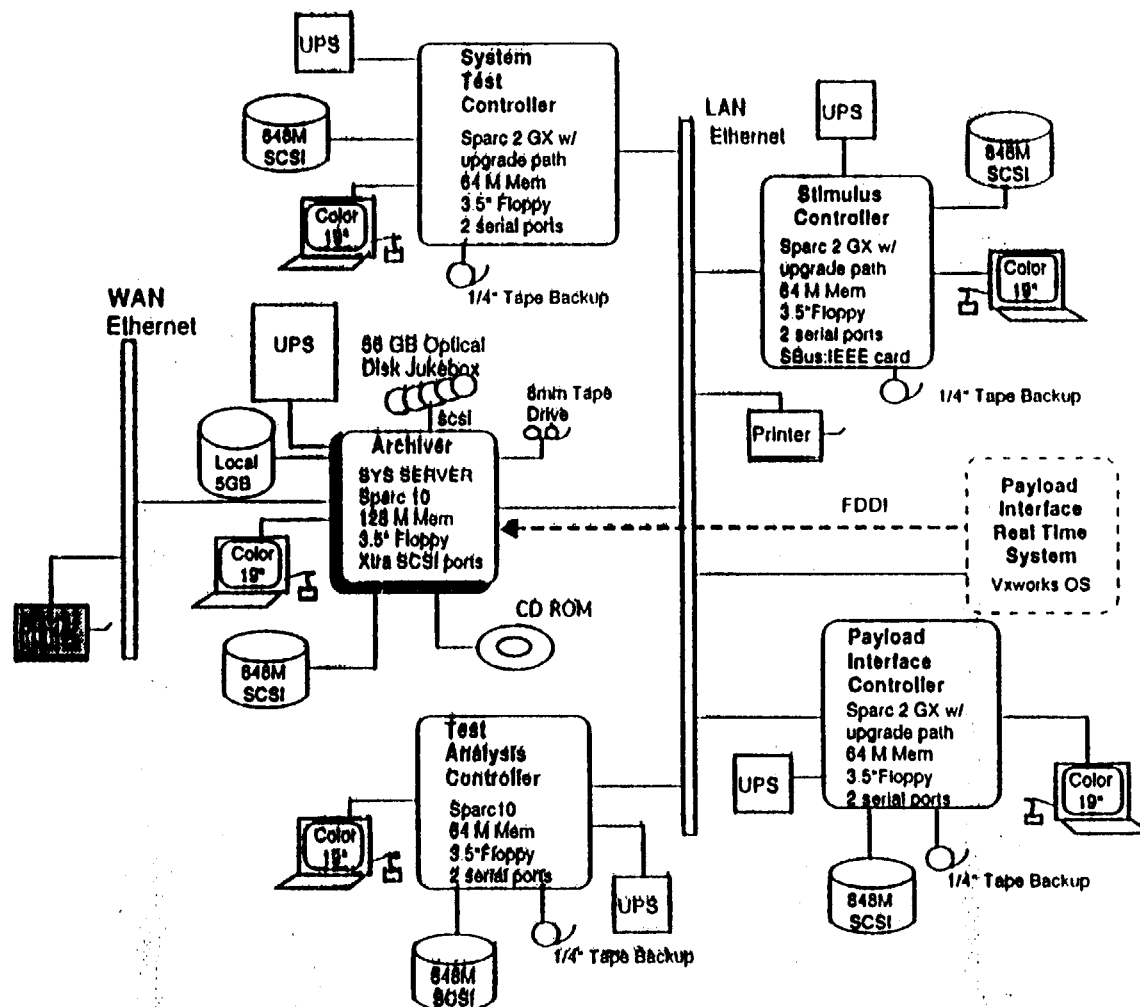




COMPUTATIONAL TOPOLOGY



SANTA BARBARA RESEARCH CENTER
a subsidiary





SANTA BARBARA RESEARCH CENTER
a subsidiary

ARC REQUIREMENTS (Cont.)



DATA STORAGE ESTIMATES

28,001 Mbytes/instrument

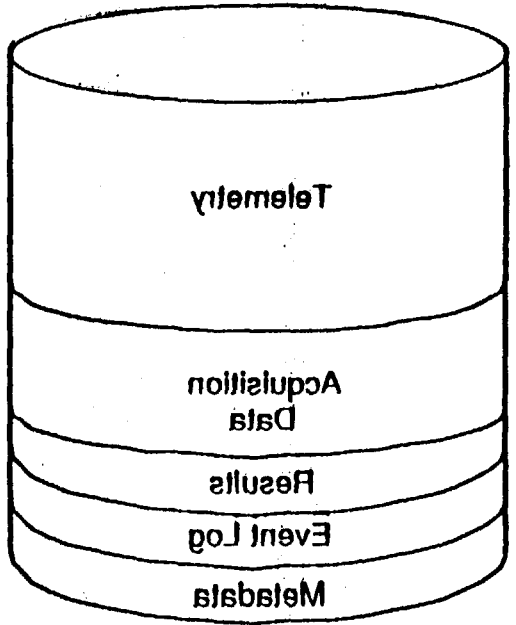
14,850 Mbytes/instrument

24 Mbytes/instrument

48 Mbytes/instrument

8 Mbytes/instrument

41 Mbytes Total/instrument

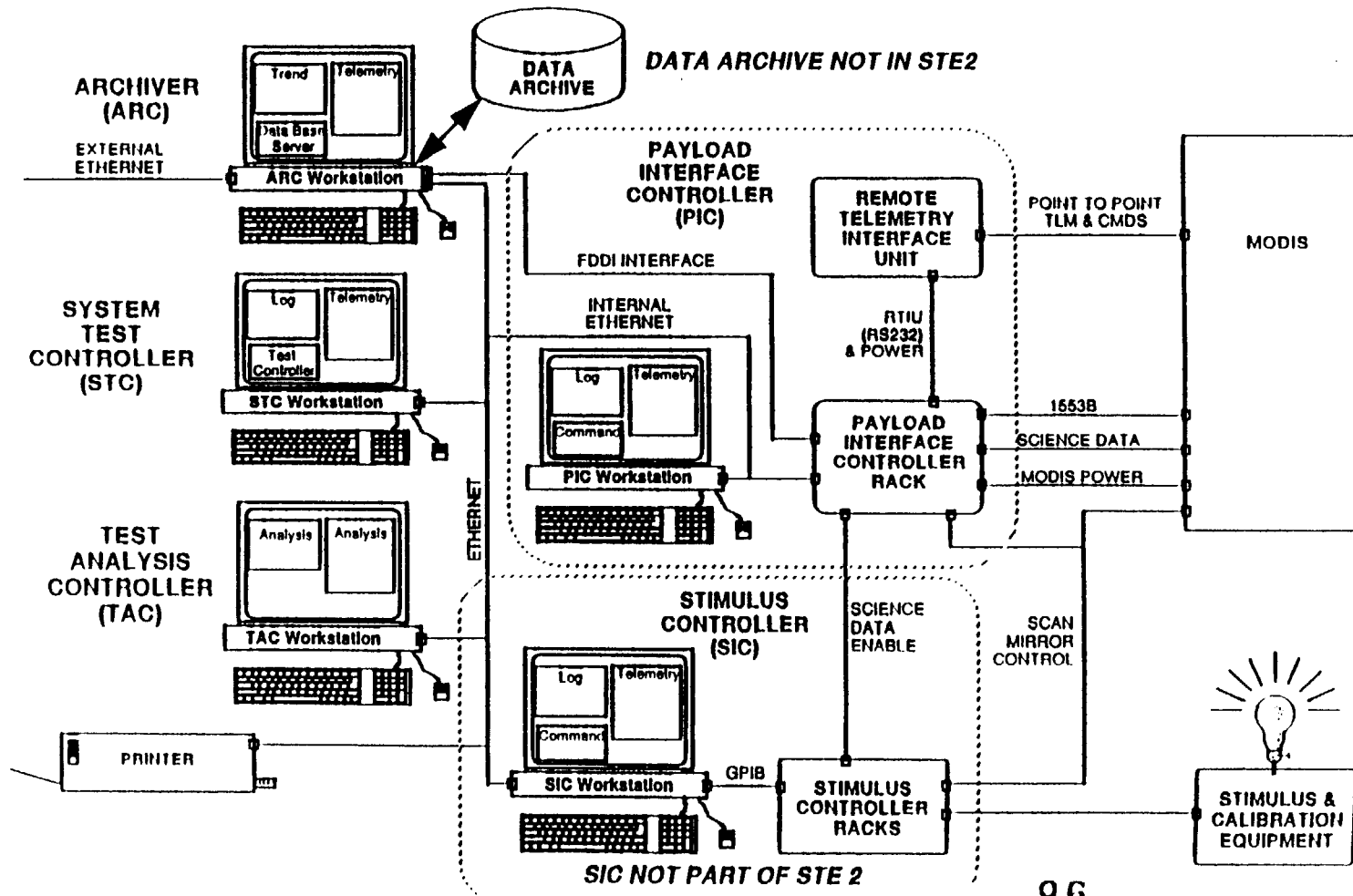




THE FIVE STE ARCHITECTURE MODULES ARE BUILT AROUND FIVE SUN WORKSTATIONS



SANTA BARBARA RESEARCH CENTER
a subsidiary



Data Retrieval Issues

Who are the MAT users?

Identify yourselves, and your needs: Real test data, v.s. Simulated data
Complete data stream v.s. partial
Trend data/archive v.s. Real time

What does the MAT system have to do? Current thinking is that it is our intention to "duplicate" the Test Analysis Controller.

Data transfer will be by overnight delivery of 8mm tape backup, contents are TBD.

This is not a "real time" system, and it is subject to SBRC data editing.

Data format will be dependent on SBRC GSE software, and does not necessarily reflect how any other software will format the data